

## N O T I C E

THIS DOCUMENT HAS BEEN REPRODUCED FROM  
MICROFICHE. ALTHOUGH IT IS RECOGNIZED THAT  
CERTAIN PORTIONS ARE ILLEGIBLE, IT IS BEING RELEASED  
IN THE INTEREST OF MAKING AVAILABLE AS MUCH  
INFORMATION AS POSSIBLE

# RESEARCH AND TECHNOLOGY

## ANNUAL REPORT 1981

(NASA-TM-84158) RESEARCH AND TECHNOLOGY  
REPORT, 1981 (NASA) 81 P HC A05/ME A01

N82-21110

CSCI 05A

G3/85  
Unclas  
16888



George C. Marshall  
Space Flight Center  
Research and Technology Office

**ANNUAL REPORT**

**1981**

**RESEARCH and TECHNOLOGY**

**Prepared by the**

**Research and Technology Office  
Science and Engineering Directorate  
GEORGE C. MARSHALL SPACE FLIGHT CENTER**

# TABLE OF CONTENTS

	PAGE
INTRODUCTION.....	1
SCIENCE AND APPLICATIONS.....	1
Solar Physics.....	1
Solar Maximum Mission.....	1
Ultraviolet Spectrometer and Polarimeter.....	2
Coronagraph/Polarimeter.....	3
Solar Magnetic Fields.....	3
Solar Structure, Dynamics, and Activity.....	6
Global Meridional Flow.....	6
Penumbral Structures.....	8
Solar Activity Relationships.....	8
Precise Measurement of Total Solar Irradiance.....	8
Magnetospheric Physics.....	10
Magnetospheric Plasma Characteristics.....	10
Retarding Ion Mass Spacetrometer.....	10
Light Ion Mass Spectrometer.....	12
Thermal Plasma Modeling.....	14
Graphical Presentation of Low-Energy Plasma.....	15
Spacecraft-Plasma Interactions.....	16
Plasma Flow Studies.....	18
Optical Observations of Magnetosphere/ Atmosphere Coupling.....	20
Planetary Plasma Processes.....	22
Jupiter.....	23
Saturn.....	24
Astronomy.....	26
Optical Astronomy.....	26
X-Ray Astronomy.....	26
Gamma-Ray Astronomy.....	27
Cosmic Ray Research.....	29
Atmospheric Sciences.....	31
Sensor Evaluation and Mesoscale Program.....	31
Mesoscale Research.....	32
Ionosphere-Severe Storms Coupling.....	32
Lightning Research.....	33
Cloud Physics.....	33
Global Weather Satellite Studies.....	34
Fifth Annual Workshop on Aviation Meteorology Research.....	35
Shuttle Turbulence Simulation.....	36
Design of the Atmospheric General Circulation Experiment (AGCE) for Spacelab Flights.....	36



## TABLE OF CONTENTS

### SCIENCE AND APPLICATIONS CONT'D

	PAGE
Materials Processing in Space.....	38
Crystal Growth.....	38
Melt Growth.....	38
Vapor Transport.....	39
Solution Growth.....	39
Metals, Alloys, and Composites.....	40
Monotectic Alloys.....	40
Eutectic Systems.....	40
Casting Experiments.....	40
Containerless Processing.....	41
Glass Fining.....	41
Containerless Technology Demonstrations.....	41
Electrophoresis.....	41
SPACE SYSTEMS DEFINITION.....	42
Ground Launched Transportation Systems.....	42
Orbital Transfer Vehicles.....	43
Solar Electric Propulsion System.....	44
Teleoperator Maneuvering System/Remote	
Satellite Servicer.....	45
Command and Telemetry Link.....	46
Signal Processor for FM-CW Radar.....	47
Gravity Probe B.....	47
Advanced X-Ray Astrophysical Facility.....	48
Pinhole Occulter Facility.....	49
Tethered Satellite System.....	50
Large Space Systems.....	51
Space Platform.....	52
User Requirements.....	53
Manned Space Platform.....	53
Deployable Platform Activities.....	54
Deployable Antenna Flight Experiment.....	55
Very Long Baseline Interferometry	
Experiment.....	56
Experimental Geostationary Platform.....	57
SPACE TECHNOLOGY.....	58
Chemical Propulsion Systems.....	58
Shuttle External Tank.....	58
Automation of Solid Rocket Design.....	59
Shuttle Solid Rocket Motor Nozzle	
Ablative Evaluation.....	59
Concentric-Chamber, Dual-Throat Thrust	
Chamber.....	60

## TABLE OF CONTENTS

### SPACE TECHNOLOGY CONT'D

	PAGE
Materials and Processes.....	61
Combined Specular/Diffuse Surface	
Thermal Technology Advancement.....	61
Acoustic Environmental Accuracy Requirements	
for Response Determination.....	62
Second Generation Sprayable Ablator	
for Solid Rocket Booster.....	62
Multilayer Insulation System.....	63
Evaluation of Corrosion Protective	
Systems on Aluminum.....	63
Electron Beam Weld Model.....	64
Variable Polarity Plasma Arc Welding.....	64
Micro-Accurate Weld Arc Control	
Development.....	65
Detection of Residual Silicone	
Contaminants on Bonding Surfaces.....	65
Electrical Power Technology.....	67
Power System Automation.....	67
Power System Controller for Large Space	
Electrical Power Systems.....	67
High Voltage Battery.....	68
Thermophotovoltaics.....	68
Solar Cell Characterization.....	69
Electronics.....	70
High Density Electronics.....	70
Interactive Graphics Design.....	70
Optical Array Sensor.....	70
Three Phase Motor Controller.....	71
Ground Loop Opto-Isolation.....	72
Superconductivity Research.....	72
Readout Circuitry for the	
GP-B Experiment.....	72
Evaluation and Analysis of	
Superconducting Composites.....	73

## ILLUSTRATIONS

FIGURE	TITLE	PAGE
1.	Longitudinal Magnetogram and Intensity Plot with Overlay of UVSP Field of View.....	4
2.	Observed Magnetic Field Structure with Outline of Umbral and Penumbra Borders.....	4
3.	Observed Sunspot with Table of Calculated Vertical Gradients (Active Region 2744).....	5
4.	Observed Poleward Migration of the Mean Latitude of Three Bands of Filaments and Its Relation to the Global Magnetic Field Pattern.....	7
5.	Sunspot Photograph from Big Bear Solar Observatory.....	7
6.	Large Flare Frequency versus Sunspot Number.....	9
7.	CCR Frequency as a Function of Aperture Area.....	10
8.	Data Obtained from Various RIMS Operating Modes.....	11
9.	Two Views of the Relationship Between the Plasmasphere and Plasmasheet Derived from ISEE Data.....	13
10.	Thermal Plasma Characteristics along the Orbit of the SCATHA Satellite.....	13
11.	Rapid Spin Phase Versus Energy Spectrograms Obtained From ISEE.....	15
12.	Potential Contours for a Spherical Satellite Geometry with a Differential Potential Across the Spacecraft.....	17
13.	Differential Ion Flux Probe.....	19
14.	Use of a Tethered Test Body to Conduct Plasma Experiments.....	20

# ILLUSTRATIONS CONT'D

FIGURE	TITLE	PAGE
15.	Fabry-Perot Optical and Detection Assemblies.....	21
16.	Voyager Observations of Natural Radio Emissions from the Jovian Magnetosphere.....	24
17.	Electron Densities in the Ionosphere of Saturn obtained from Model Calculations and the Pioneer and Voyager Spacecraft.....	25
18.	Trajectories of the Two Balloons Launched on October 6 - 7, 1980.....	28
19.	Pulse Profile from The Crab Nebula, NP0532, from the October 1980 Balloon Flight.....	28
20.	Cosmic-Ray Instruments Being Prepared for the October 1980 Balloon Flight.....	30
21.	Warm Cloud Physics Experiment on the KC-135 Aircraft (Front Center Pallet).....	35
22.	Shuttle-Derived Launch Vehicle Concepts Being Studied at MSFC.....	42
23.	Orbital Transfer Vehicle.....	43
24.	Solar Electric Propulsion Stage.....	44
25.	Teleoperator Maneuvering System.....	45
26.	Gravity Probe B.....	48
27.	Advanced X-Ray Astrophysical Facility.....	49
28.	Pinhole Occulter Facility.....	50
29.	Tethered Satellite System.....	51
30.	Space Platform.....	52
31.	Manned Space Platform.....	54

# ILLUSTRATIONS CONT'D

FIGURE	TITLE	PAGE
32.	Expandable Large Space Structures.....	55
33.	Very Long Baseline Interferometry Using a Deployable Antenna.....	56
34.	Experimental Geostationary Platform.....	57
35.	Uncooled Dual Throat Test Rocket Engine.....	61
36.	Variable Polarity Plasma Arc Welding.....	64
37.	Weld Arc Control with CID Sensor.....	66
38.	Power System Controller Block Diagram.....	67
39.	Thermophotovoltaic Generator Module.....	69
40.	High Speed Interactive Color Graphic Design Station.....	71

## INTRODUCTION

Although the primary roles of the Marshall Space Flight Center are those of developing propulsion systems, large complex payloads and large space systems, the Center pursues a strong program of research and technology. As is evident from review of the varied tasks, each of them either has a high probability of application to current or future programs or is an application of the results of current programs. Collaboration with the academic and industrial communities continues to be dedicated team effort, beneficial to each of the participating parties.

In keeping with the request of the Deputy Administrator, this year's report provides the names of responsible Center personnel, their respective organization correspondence code and commercial telephone number. Also, the more significant publications are listed following each individual accomplishment. Where there has been contractor or university involvement with the task, this is also indicated in the report. Additional information concerning a task may be obtained either from the identified responsible individual or from the Research and Technology Office (correspondence code ERO1, MSFC, AL 35812; telephone 205-453-1023). Additional copies of this report may also be obtained from the Research and Technology Office.

## SCIENCE AND APPLICATIONS

### SOLAR PHYSICS

Solar activity continues to pose questions of fundamental importance to the understanding of solar physics. With solar activity at a very high level during the last year, solar physics research at MSFC has centered on basic problems related to different observable manifestations of solar activity; viz., sunspots, flares, the active corona, and large-scale mass motions. In addition, new technologies have been explored in designing instruments to better study the solar irradiance and solar X-ray radiation.

### Solar Maximum Mission

The Solar Maximum Year (SMY), an international science program to study the Sun which involves the coordination of space-borne and ground-based observations of solar activity, ended February 28, 1981. MSFC contributed importantly to the SMY program through its magnetograph observations, its Ultraviolet Spectrometer and Polarimeter (UVSP) experiment on the Solar Maximum Mission, and the Coronagraph/Polarimeter SMM instrument.

## Ultraviolet Spectrometer and Polarimeter

The UVSP experiment, which obtains information about the solar atmosphere in ultraviolet light, continued observations until the spacecraft attitude control system failed in November 1980. The ultraviolet part of the electromagnetic spectrum, unobservable from the ground, allows study of the transition zone between the Sun's lower atmosphere (the chromosphere) and its upper atmosphere (the corona). The addition of a rotating polarizer in the optical train of this instrument also allows measurement of the polarization of the light. These measurements allow the determination of the characteristics of the solar magnetic field. Data reduction and scientific data analysis have progressed steadily.

For example: Circular polarization in a solar transition region emission line was observed. This is interpreted as evidence of a magnetic field producing Zeeman effect in the region where the line is formed. Over a sunspot, the field (1) has peak values over the umbra of the sunspot, (2) has a range from approximately 1000 to 1400 gauss (statistically significant values), and (3) agrees in polarity with the photospheric field in the same spot as observed by the MSFC solar observatory.

Studies of certain spectral lines emitted by the transition-region plasma permit the determination of densities in this important part of the solar atmosphere. The spatial and temporal evolution of the Si IV, O IV intensity, density, and mass motions in the preflare and flare transition-zone plasmas were studied. The density is determined from the observed intensity ratio between the Si IV resonance line and the O IV intersystem line. The principal results are: (1) The EUV flare observed on April 8, 1980, in the Si IV and O IV lines is unambiguously identified as occurring in a low-lying pre-existing transition-zone loop. The loop spanned the magnetic neutral line which separated a larger leader spot and a newly emerged isolated spot of opposite polarity. The loop became observable some 20 minutes before it flared. It underwent slow brightness changes along its entire length, with the most prominent changes at the top portion of the loop and at its westernmost footpoint near the leader spot. (2) At the onset of the flare, the easternmost footpoint, which was anchored in an isolated spot region of high longitudinal magnetic field gradient, suddenly showed impulsive brightening with large intensity increases. This was correlated with an impulsive hard X-ray burst observed at the same time. This flaring kernel had previously been inconspicuous. (3) The density of the transition-zone plasma at a temperature of approximately  $10^5$  K at the flaring footpoint increased an order of magnitude from its preflare value of  $2 \times 10^{11} \text{ cm}^{-3}$  to  $3 \times 10^{12} \text{ cm}^{-3}$  during the impulsive brightening. (4) The large intensity and density increases in the flaring kernel were associated with a downward mass motion with a velocity of approximately  $20 \text{ km s}^{-1}$ .

Another significant new observation pertains to transition-region oscillations in sunspots. Time-series observations of the profile of the C IV resonance line 1548.19 have been obtained in eight sunspots. All of the sunspots display significant oscillations in line-of-sight velocity with frequencies in the range 5.8 to 7.8 mHz (periods of 129 to 173 s). Significant intensity oscillations were observed at the same periods in four of the time series; the maximum intensity is in phase with maximum blue shift.

Difference spectroheliograms ("Dopplergrams") of the two halves of the C IV line, as well as observations in the Si IV resonance line at 1402.77 Å and the O IV intersystem line at 1401.16 Å, also display velocity oscillations at similar frequencies, but only over sunspots. Estimates of the intensity variations (approximately 10 percent) expected from adiabatic acoustic waves with the observed velocity amplitudes ( $0.8 \text{ km s}^{-1}$  to  $3.5 \text{ km s}^{-1}$ ) are in reasonable agreement with the measured intensity amplitudes (6 to 9 percent). Current models of umbral oscillations, however, do not satisfactorily describe the observations in terms of the propagation of acoustic waves upward through the transition region. (E. Tandberg-Hanssen/205-453-0027)

### Coronagraph/Polarimeter

Research on coronal transients emphasized several aspects of these fascinating phenomena. A Skylab-era transient that occurred in association with a  $5000 \text{ km s}^{-1}$  Type II radio burst was investigated with T. Gergely and M. Kundu of the University of Maryland. The source of the radio burst traveled outward 6 or 7 times faster than did the ejected mass and, thus, into as-yet-undisturbed corona. The assumption that the source of radio emission was a weak MHD shock leads to the result that the ambient coronal magnetic field was approximately 10 G at a height of  $2.9 R_{\odot}$ , an unexpectedly large value. This calls into question the emission mechanism commonly assumed for Type II bursts.

Another study during 1981 has shown that the frequency of occurrence of solar coronal transients at maximum phase of the solar activity cycle is about the same as at minimum phase. This result is surprising, since the values of conventional indices of solar activity--e.g., sunspot number, frequency of flare occurrence, 10.7 cm radio flux, etc.--at maximum phase are integer multiples of the minimum phase values. Nonetheless, that coronal transients are associated with common types of solar activity is shown by the fact that at maximum phase transients typically occur at higher latitudes than at minimum, the same pattern exhibited by active regions, flares, etc. (E. Hildner/ES52/205-453-0123)

Gergely, T. E., Kundu, M. R., and Hildner, E.: A Coronal Transient Associated with a High Speed Type II Burst. Astrophys. J. (in press).

### Solar Magnetic Fields

During 1981 the MSFC Magnetograph program was focused on the Solar Maximum Mission (SMM) Guest Investigation with major activities in analyses of data obtained during the operational phase of SMM. A primary effort has been the study of the three-dimensional vector magnetic field of a sunspot. A coordinated sunspot observing program used MSFC vector magnetograph data to map, quantitatively, the photospheric vector field and SMM Ultra Violet Spectral Polarimeter (UVSP) magnetograph mode data to obtain the transition region line-of-sight component of the field. Figures 1 & 2 indicate the observed sunspot and the measured photospheric field; in Figure 3 the derived vertical gradients are shown for the area covered by the UVSP raster. These data are unique in that such observations of a sunspot's magnetic field have never before been obtained simultaneously. A second



ORIGINAL PAGE  
BLACK AND WHITE PHOTOGRAPH

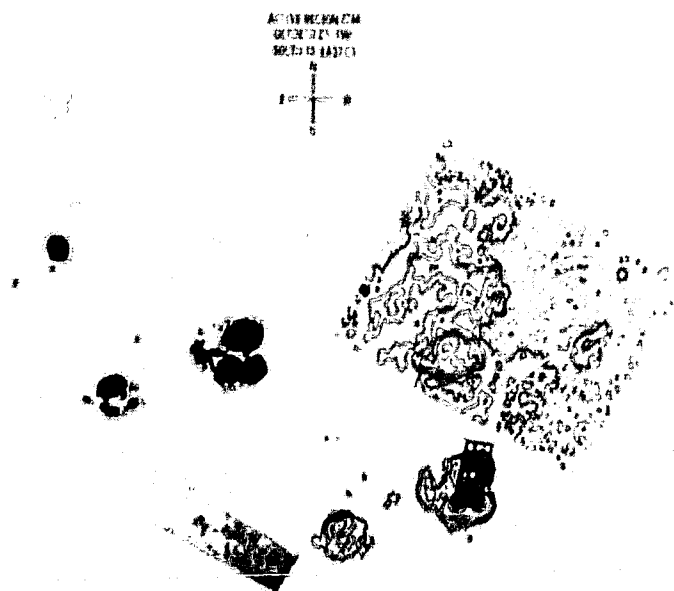


Figure 1. Longitudinal Magnetogram and Intensity Plot with Overlay of UVSP Field of View.

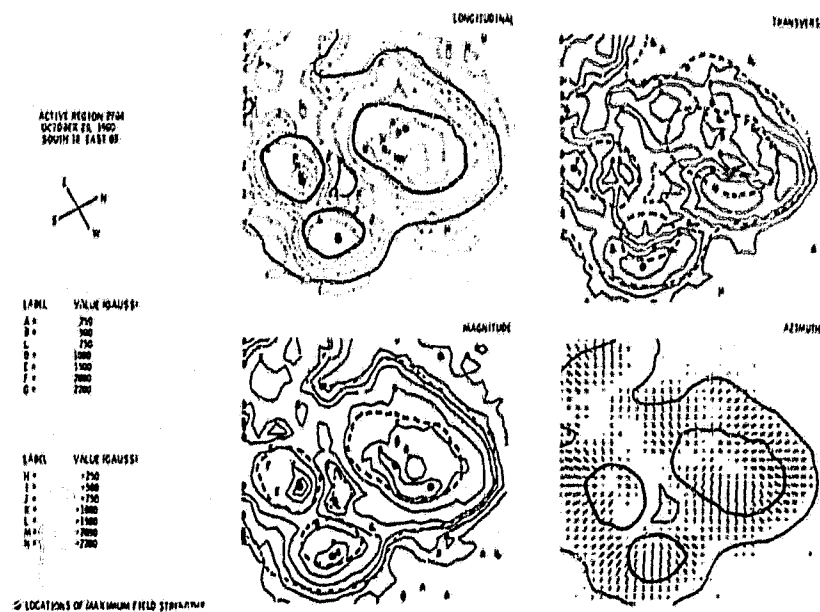


Figure 2. Observed Magnetic Field Structure with Outline of Umbral and Penumbral Borders.

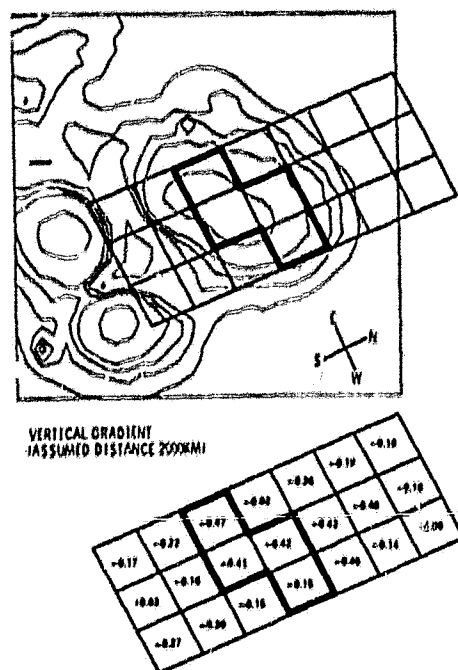


Figure 3. Observed Sunspot with Table of Calculated Vertical Gradients (Active Region 2744).

major effort was the study of flare energy buildup in magnetic fields as they are sheared by sunspot proper motions. A coordinated program with two of the SMM Investigator Teams is underway to study an active region observed on September 23, 1980. Data from the MSFC magnetograph, SMM UVSP and X-Ray Polychrometer (XRP) instruments, as well as a Lockheed rocket flight are being analyzed to obtain a self-consistent model of this region. Other analyses include: (1) a study of magnetic delta-configurations (sunspot areas of complex magnetic field structure which are frequent flare sites); (2) a study of UV bright points observed around sunspots and their relation to the sunspot's vector magnetic field structure; (3) a generalized force-free magnetic energy computation using measured transverse magnetic fields; (4) an initial analysis of flare-related transverse magnetic field changes in large flares; and (5) a study of magneto-optical effects in sunspots using coordinated observations with the MSFC magnetograph and High Altitude Observatory (HAO) Stokes polarimeter. Major efforts in MSFC support of post-mission SMM data analysis were participation in SMY Study of Energy Release in Flares (SERF) and Flare Buildup Study (FBS) Working Groups and in providing vector magnetic field data to these groups as well as to the SMM investigation Teams. MSFC Solar Observatory Reports covering the SMM operational phase were distributed to the Principal Investigators and other solar observatories. As is evident from the following publications, which resulted from the foregoing activities, quite significant results have

already been obtained. (M. Hagyard/ES52/205-453-0116)

Hagyard, M. J., Low, B. C., and Tandberg-Hanssen, E.: On the Presence of Electric Currents in the Solar Atmosphere. I: A Theoretical Framework. Solar Physics (in press).

Hagyard, M. J., West, E. A., Tandberg-Hanssen, E., Smith, J. E., Henze, W., Beckers, J. M., Bruner, E. C., Hyder, C. L., Gurman, J. B., Shine, R. A., and Woodgate, B. E.: The Photospheric Vector Magnetic Field of a Sunspot and Its Vertical Gradient. Proceedings of the Sacramento Peak Observatory Summer Workshop on the Physics of Sunspots, 1981 (in press).

Krall, K. R., Smith, J. B., Hagyard, M. J., West, E. A., and Cumings, N. P.: Vector Magnetic Field Evolution and Associated Photospheric Velocity Shear within a Flare-Productive Active Region. Solar Physics (in press).

Patty, S. R. (NASA Graduate Student Research Fellow): Analysis of the Vector Magnetic Fields of Complex Sunspots. Proceedings of the Sacramento Peak Observatory Summer Workshop on the Physics of Sunspots, 1981 (in press).

Hagyard, M. J., Cumings, N. P., West, E. A., and Smith, J. E.: The MSFC Vector Magnetograph. I: Description and System Performance. Solar Physics (submitted).

Hagyard, M. J., and West, E. A.: The MSFC Vector Magnetograph. II: Techniques for Quantitative Interpretation of Data. Solar Physics (submitted).

Schmahl, E. J., Kundu, M. R., Strong, K. T., Bentley, R. D., Smith, J. B., and Krall, K. R.: Inferences About Active Region Magnetic Fields from Simultaneous VLA Microwave Mass, X-Ray Spectroheliograms and Magnetograms. Solar Physics (submitted).

### Solar Structure, Dynamics, and Activity

#### Global Meridional Flow

MSFC, California Institute of Technology, and Mt. Wilson Observatory personnel have discovered new evidence to confirm the presence of a global meridional circulation in the solar convection zone. The evidence is a long-term poleward drift of H-alpha filaments (measured from H-alpha synoptic charts published by NOAA in Solar-Geophysical Data), which was found to be synchronous with the poleward drift of global magnetic flux patterns from the past 13 years of Mt. Wilson full-disk magnetograms (Figure 4). These data show that the surface layer of the Sun at mid-latitudes ( $20^\circ - 70^\circ$ ) flow poleward at roughly  $20 \text{ m s}^{-1}$ . This flow must be balanced by a return equator-ward flow in deeper layers. The meridional circulation, in combination with the Sun's differential rotation may be a basic driver of solar magnetic activity cycle. Data analysis is continuing to discover what the basic driver of the circulation may be. (R. Moore/ES52/205-453-0116)

ORIGINAL PAGE  
BLACK AND WHITE PHOTOGRAPH

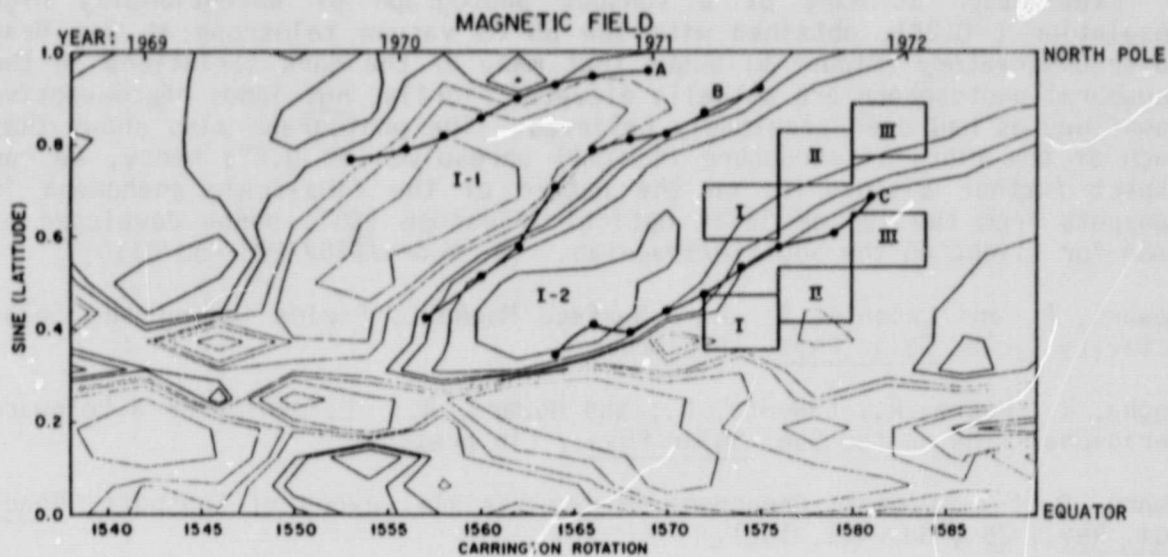


Figure 4. Observed Poleward Migration of the Mean Latitude of Three Bands of Filaments and Its Relation to the Global Magnetic Field Pattern.

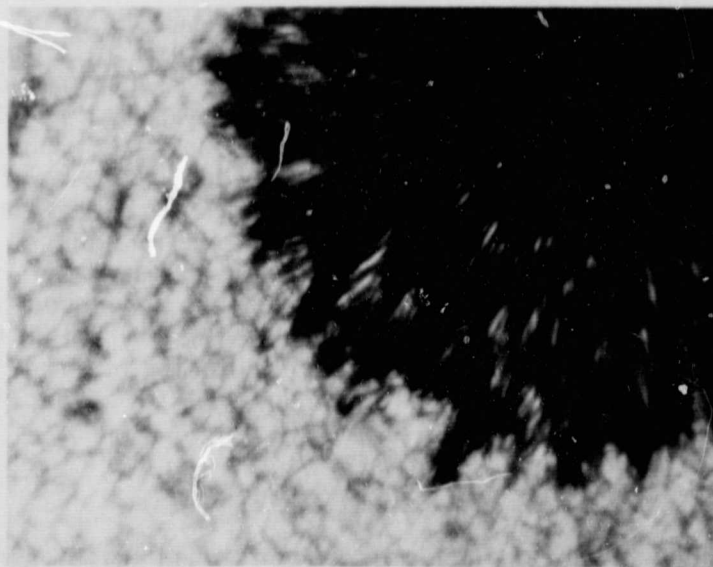


Figure 5. Sunspot Photograph from Big Bear Solar Observatory

## Penumbral Structures'

Examination at MSFC of a sunspot photograph of exceptionally high resolution (0.2"), obtained with the 65 cm vacuum telescope at Big Bear Solar Observatory (Figure 5) shows that many of the dark striations in the penumbral photosphere are actually elevated fibrils, not lanes of convective downflow, as had been previously believed. The photograph also shows that much of the fibrillar structure is still unresolved at 0.2"; hence, we can expect further discoveries on the nature of the fine-scale phenomena in sunspots from the 125 cm Solar Optical Telescope (SOT) being developed by NASA for flight on the Shuttle/Spacelab. (R. Moore/ES52/205-453-0116)

Howard, R. and LaBonte, B. J.: Surface Magnetic Fields During the Solar Activity Cycle. Solar Phys., (in press).

Tophu, K.; Moore, R.; LaBonte, B.; and Howard, R.: Evidence for a Poleward Meridional Flow on the Sun. Solar Phys., (in press).

Moore, R. L.: Dynamic Phenomena in the Visible Layers of Sunspots. Space Sci. Rev., **28**, 387-421, 1981.

Moore, R. L.: Structure of the Sunspot Penumra. Astrophys. J., **249** (in press).

Moore, R. L.: Dynamic Phenomena in Sunspots. Proceedings of the Sacramento Peak Observatory Summer Workshop on the Physics of Sunspots, L. Cram and J. Thomas (eds.) (in preparation).

## Solar Activity Relationships

An examination at MSFC of the characteristics of solar flares, using data reported in NOAA's Solar-Geophysical Data (published by World Data Center A for Solar-Geophysical Data), reveals that the relation between two conventional indices of solar activity may vary with phase in the solar cycle. Figure 6 shows that during the ascending phase of solar cycle 21 there was one (or perhaps two) linear relation(s) between the number of flares of importance  $> 1$  per month and the monthly sunspot number. Around the time of solar cycle, i.e., sunspot number maximum, this relation changed abruptly, so that the same number of sunspots produced 40 percent more flares. The relatively abrupt departure from a relation that had endured for some 40 months is unexplained. Investigations aimed at understanding this result and whether the pattern is repeated for other solar cycles are continuing. (R. Wilson/ ES52/205-453-0116)

## Precise Measurement of Total Solar Irradiance

MSFC research in solar radiometry continued with further laboratory testing of a crystal cavity radiometer (CCR) as an advanced radiometric sensor concept. By monitoring the frequencies of a thermally controlled reference quartz crystal and an exposed, black-coated crystal enclosed in a retroreflecting cavity, the measurement of solar flux variations is reduced

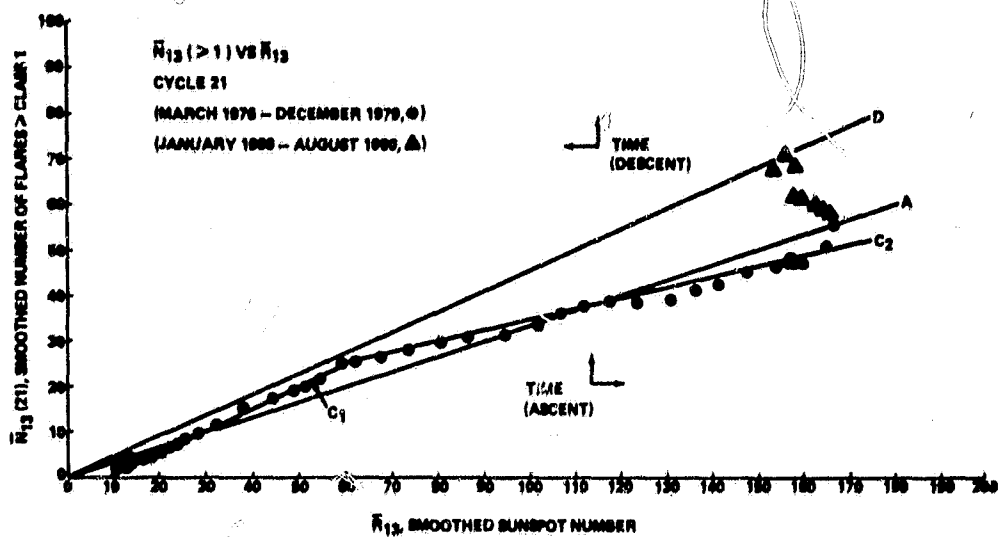


Figure 6. Large Flare Frequency versus Sunspot Number

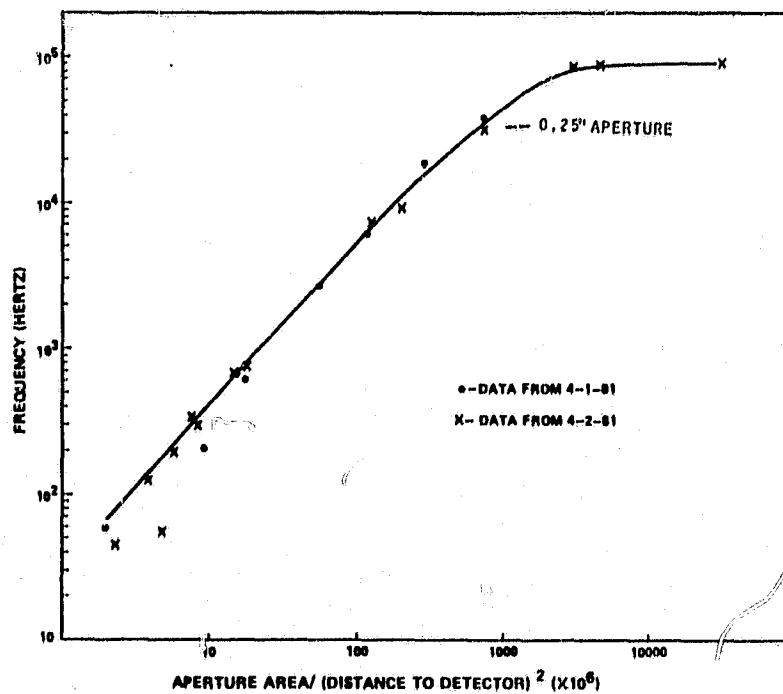


Figure 7. CCR Frequency as a Function of Aperture Area

to monitoring changes in beat frequency. Technical aspects of the radio-meter's design were investigated, including the optimum aperture size. From data shown in Figure 7, it was determined that the CCR frequency is a linear function of aperture size up to an aperture of approximately 0.1 cm. Therefore, a 0.1 cm aperture is appropriate to optimize frequency output while minimizing field-of-view noise from the atmosphere and other effects. (M. Hagyard/ES52/205-453-0116)

## MAGNETOSPHERIC PHYSICS

### Magnetospheric Plasma Characteristics

Magnetospheric low-energy plasma study is a dominant part of the MSFC space plasma physics activities. Data are currently being collected and analyzed from three different spacecraft, the Spacecraft Charging at High Altitudes (SCATHA) satellite, the International Sun-Earth Explorer (ISEE) satellite, and the Dynamics Explorer-1 (DE) satellite. A great number of fundamental discoveries concerning the origin and energization of this low energy component have been made during the past year. In addition, the successful launch of the DE spacecraft promises a wealth of new information on the interchange of ionization between the magnetosphere and ionosphere.

### Retarding Ion Mass Spectrometer

The two Dynamics Explorer spacecraft were launched into coplanar polar orbits on August 3, 1981. The DE-1 spacecraft contains six plasma and field instruments which included the MSFC Retarding Ion Mass Spectrometer (RIMS). The DE-1 orbit of 569 km perigee by 23,173 km apogee is ideal for sampling the inner magnetosphere. The RIMS instrument combines the energy analysis capabilities of a retarding potential analyzer with the mass analysis capabilities of a magnetic ion mass spectrometer. In the inner plasmasphere and ionosphere, the RIMS instrument will measure the bulk thermal plasma parameters of density, temperature, and flow. In the outer plasmasphere, the narrow angular acceptance of the detector oriented perpendicular to the spacecraft spin axis will permit the determination of the ion pitch angles or angle with respect to the Earth's magnetic field.

ORIGINAL PAGE  
BLACK AND WHITE PHOTOGRAPH

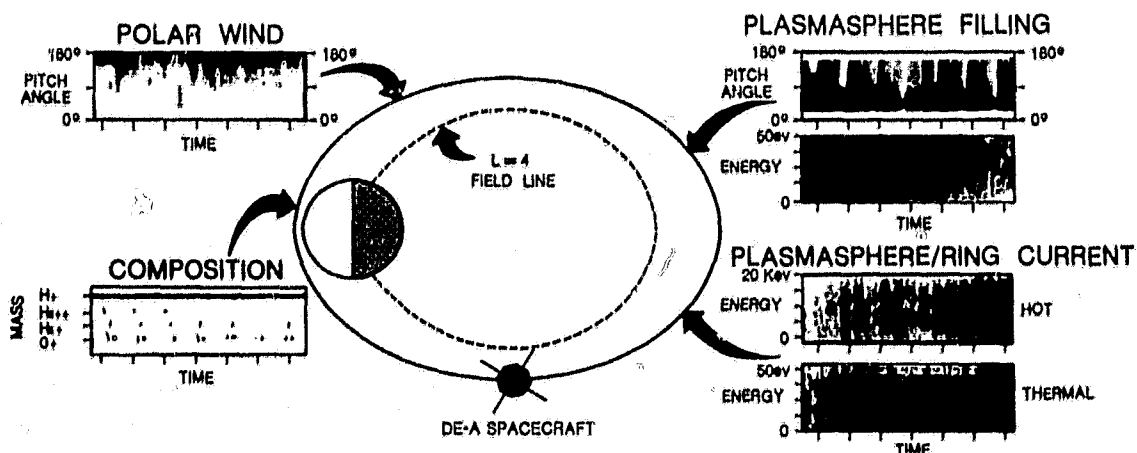


Figure 8. Data Obtained from Various RIMS Operating Modes

Calibration of the three RIMS detectors was completed in the MSFC thermal plasma vacuum facility during this year just prior to launch. At this time, the RIMS instrument is operating successfully in orbit. Final checkout of the instrument and conditioning of the electron multiplier is in process. The instrument operations have been scheduled for the first three months to begin at the end of conditioning. Examples of the RIMS science investigations are shown in Figure 8. Early data from the instrument have shown the dynamic nature of the plasmopause response to changing magnetic activity as well as the different plasma temperatures which can be found throughout the plasmasphere.

With regard to the origin of thermal plasma, the ISEE-1 mass spectrometer has observed  $H^+$ ,  $He^+$ ,  $O^+$ ,  $He^{++}$ , and  $O^{++}$  ionic species within the magnetosphere. The latter four ions are far more abundant in the Earth's upper atmosphere than in the solar wind, and it now appears certain that the major portion of observed low-energy magnetosphere plasma is of Earth, rather than solar, origin. The  $O^{++}$ , and perhaps  $He^{++}$ , which have only recently been found in significant amounts within the Earth's plasmasphere, are believed to result from enhanced thermal diffusion of these ions from the Earth's upper atmosphere upward along magnetic field lines.



Evidence for transport of the low-energy plasma were seen in both directions along the magnetic field direction as well as by convection perpendicular to the magnetic field. Impulsive surges convecting thermal plasma away from the plasmasphere were observed during the initial phase of a substorm. Also, as shown in Figure 9, ISEE-1 observations indicate cool (1-2 eV) flows of  $H^+$  and  $He^+$  moving up from the ionosphere to fill the outer region of the plasmasphere during magnetically quiet periods.

New evidence for perpendicular energization of thermal ions was found in angular flux distributions with peak fluxes either perpendicular to the magnetic field direction (called pancake or trapped distributions) or between the directions parallel and perpendicular to the magnetic field direction (called conics). Both types of distributions are believed to occur when these ions are perpendicularly accelerated by wave electric fields oscillating in resonance with the ions' unidirectional motions around the field. This phenomenon is believed to occur above the aurora and also in regions where hot solar-origin plasma and cold ionospheric-origin plasma are mixed.

Finally, there are been indications of the loss mechanisms for thermal plasma in plasma jets squirting out of the magnetosphere within the magnetotail along field lines presumed to be linked to the solar magnetic field. Evidence of ionospheric origin plasma conveyed to near the dayside magnetosphere boundary also indicates transport and perhaps loss across this boundary. (C. Baugher/ES53/205- 453-0029).

#### Light Ion Mass Spectrometer

The Light Ion Mass Spectrometer (LIMS) was launched on the joint DOD/NASA satellite SCATHA in February 1979 into a near-synchronous orbit. This orbit placed the LIMS in an excellent position to study the low-energy plasma populations of the plasmasphere and plasma trough regions. An example of measurements during one orbit is shown in Figure 10. Between 1730 and 2230 Local Time, the satellite was in a region of very cold plasma ( $T_i < 1$  eV) with a significant percentage of  $He^+$  ions, 5 to 10 percent. This region is shown as the dusk bulge region of the plasmasphere populated by upward diffusion from the ionosphere. At earlier and later local times, however, the satellite encountered regions of relatively warm ( $T_i > 10$  eV) plasma. Significantly, these regions had no discernible  $He^+$  ions. The distributions in pitch angle of these ions were in some regions peaked at  $90^\circ$  (trapped) and in other regions were peaked along the magnetic field lines. The significance of these observations is that they show that acceleration mechanisms are acting to populate the plasma trough regions of the magnetosphere with energized ionospheric plasma, and that these mechanisms are mass selective. Mechanisms involving resonant cyclotron interactions between particles and waves are strong candidates for explaining these mechanisms.

Data from the University of California at San Diego Plasma Instrument on SCATHA are also being analyzed in this joint study effort with the University of Alabama in Huntsville. Observations of waves and plasmas confined near the equator have demonstrated the importance of the equator as a plasma

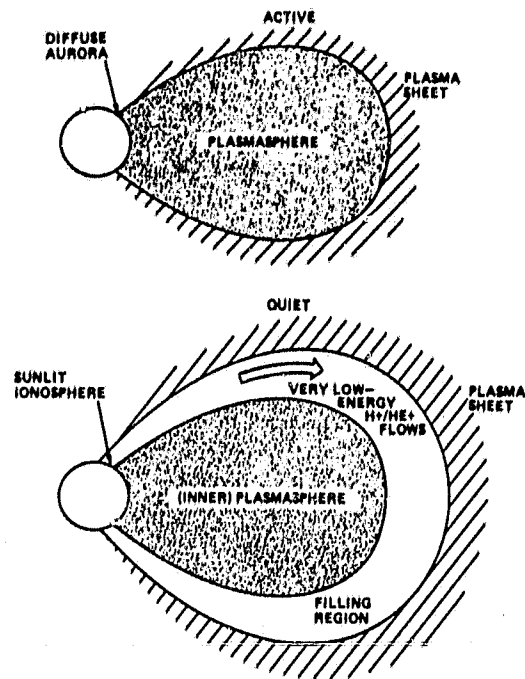


Figure 9. Two Views of the Relationship Between the Plasmasphere and Plasmasheet Derived from ISEE Data.

LIMS/SCATHA FEBRUARY 9, 1979

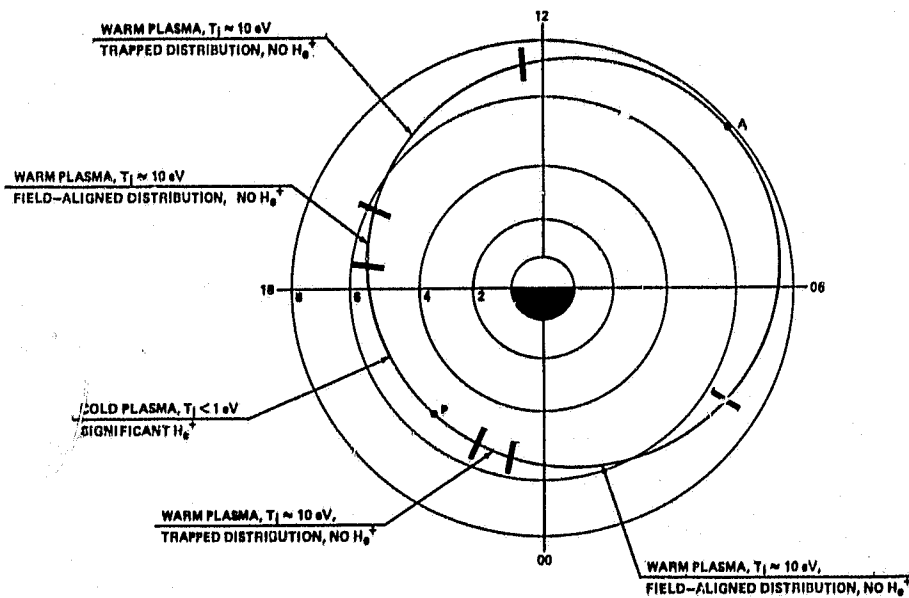


Figure 10. Thermal Plasma Characteristics along the Orbit of the SCATHA Satellite

reservoir and a site of wave-plasma interactions. A warm ion population ( $T_i$  50 eV,  $N_i$  10 ions/cm<sup>3</sup>) was found to be trapped within a few degrees latitude of the magnetic equator throughout the dayside at 5.5 to 6  $R_E$ . Observations of electromagnetic waves in the 20 to 200 Hz frequency range coincided with the trapped plasma observations, and it is likely that the plasmas and waves are causally related. These, and the observations discussed previously, show that interactions between waves and plasmas most likely play a fundamental role in magnetospheric dynamics. (D. Reasoner/ES53/205-453-3037)

### Thermal Plasma Modeling

Within the last year the development of a computer modeling program has been initiated. The first step in this program was the development of a simple diffusive equilibrium model of the plasmaspheric ions  $O^+$ ,  $H^+$ , and  $He^+$ . The 13-moment diffusion equations for the topside ionosphere developed by St. Maurice and Schunk were solved in order to investigate the role of  $He^+$  thermal diffusion in the plasmasphere. This is a topic of current research interest as a result of the large fractional concentrations of  $He^+$  ( $He^+/Total$  ion density = 0.1 - 0.5) and its effect on waveparticle interactions in the plasmasphere observed by GEOS and ISEE satellite measurements. Preliminary results indicate that steep plasmaspheric temperature gradients may explain certain anomalous situations; however, the bulk of the comparisons of model and ISEE measurements indicate that the thermal diffusion process is not adequate to explain the observed plasmaspheric  $He^+$  concentrations.

More sophisticated computer modeling techniques and simultaneous low- and high-altitude spacecraft measurements are needed to better understand the composition of the plasmasphere. To obtain adequate spacecraft measurements, additional analysis is needed of the plasmaspheric composition and temperature measurements to be obtained by the DE-1 RIMS instrument and with the low-altitude measurements of DE-2. To achieve the needed modeling goals, the MSFC group is working with Utah State University and the University of Alabama in Huntsville to incorporate existing plasma modeling programs into a sophisticated computer model of the terrestrial plasmasphere. (J. H. Waite, Jr., J. L. Horowitz/ ES53/453-3037)

Waite, J. H., Jr., and Horowitz, J. H.:  $He^+$  Thermal Diffusion in the Plasmasphere. Submitted to Geophysical. Res. Lett.

ORIGINAL PAGE  
BLACK AND WHITE PHOTOGRAPH

Graphical Presentation of Low-Energy Plasma

The revelation of the complexity of the magnetospheric low-energy plasma parameters has led to a complete re-evaluation of the analytical tools used for its study. New analytical display techniques are required to properly evaluate the validity of calculated bulk parameters ( $N$ ,  $T_i$ ,  $V_i$ ) from the data. The low-energy thermal plasma environment in the Earth's magnetosphere was, at first, believed to be completely Maxwellian in distribution

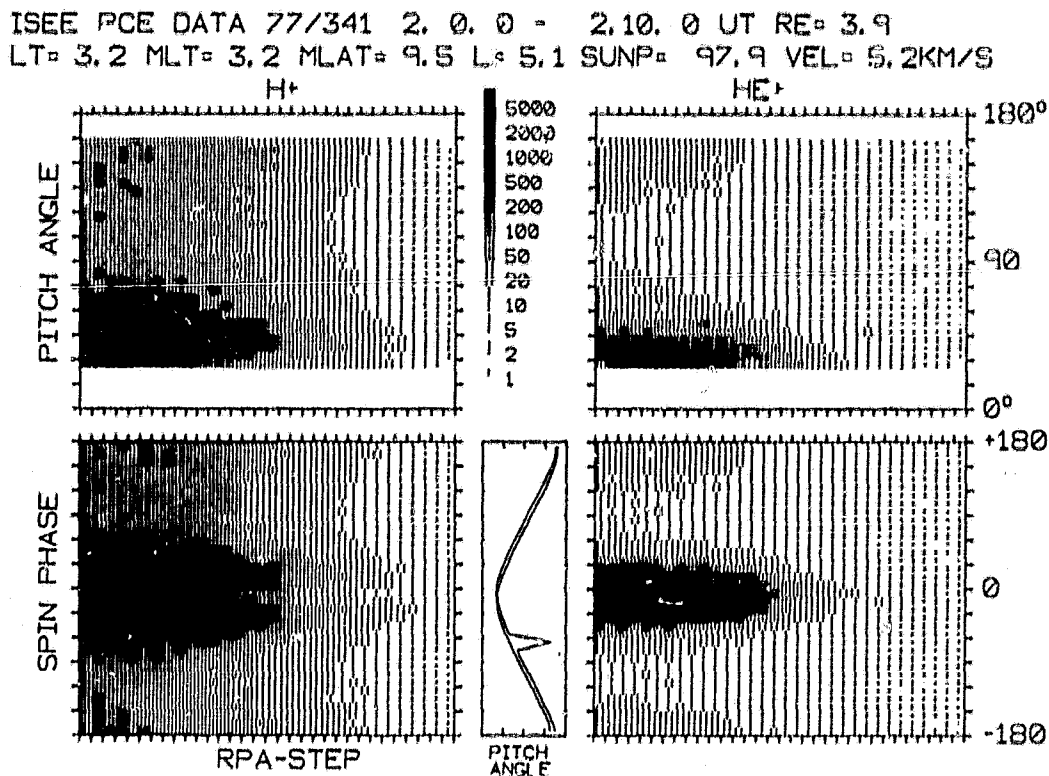


Figure 11. Rapid Spin Phase Versus Energy Spectrograms Obtained from ISEE

and ionospheric in temperature. The low-energy composition measurements from the ISEE and SCATHA spacecraft have revealed field-aligned, trapped, and conic anisotropies seen with temperatures of an order of magnitude or more above that of ionospheric plasma. Original multidimensional graphic techniques have been developed to aid in scientific analysis. Several types of spectrograms and three-dimensional contour techniques developed are now being applied to data from SCATHA and ISEE as routine production elements. Figure 11 illustrates an extremely quick (in terms of computer and plotting

time) spectrogram method used to examine the details in the angular distribution of the low-energy plasma measured from ISEE. Here the data are divided into spacecraft angle (pitch angle in the top panel) and the RPA or energy step where the corresponding counts are coded as a number of parallel bars. This method accentuates the often observed extreme differences between various magnetospheric plasma constituents (hydrogen and helium in this case). The goal of this activity is to facilitate the unveiling of low-energy plasma characteristics interactively and to have these displays available for comparison with other experimental and theoretical data sets. (J. Green/ES53/205-453-0028)

Green, J. L. and Johnson, J.: Spectrogram Techniques. (To be published as a NASA TM)

Chappell, C. R., Horowitz, J. L., Reasoner, D. L., Baugher, C. R., Craven, P. D., Green, J. L.: Low-Energy Plasma Composition Results from the ISEE and SCATHA Satellite. Ion Composition and Magnetospheric Processes, Edited by R. G. Johnson, IAGA Edinburgh General Assembly, August 1981 (in press).

### Spacecraft-Plasma Interactions

The interactions between a spacecraft and its environment, particularly the plasma population, affects spacecraft systems and plasma measurements, and can cause spacecraft failures. This interaction is best studied with plasma data. The twofold problem, therefore, is to determine the effects of such interactions on the plasma measurements and then use these measurements to study the spacecraft surface potentials, space-charge sheath, and plasma currents.

Interpretation of thermal ion data obtained from the mass spectrometer on ISEE-1 deep in the plasmasphere has focused on a thin-sheath approximation to the spacecraft-plasma interaction. This model was based on previous work by Singh and Baugher (1981) which showed that the thin-sheath approximation was appropriate for the narrow-aperture ISEE instrument. An analytic approximation has been obtained for the flux into the narrow-aperture instrument in a flowing, rammed plasma for the first time, and the resulting expression has been employed in a convergence method for curve fitting. This method is much more accurate than previous procedures which ignored sheath effects on charged spacecraft, and it is much faster than the more versatile but computationally time consuming numerical integration methods. Quantitative results from the analysis of RPA data are the ion temperature,

density, and the spacecraft potential. Simulation studies have shown that the temperature calculation is relatively insensitive to errors in the other two parameters. The ion density and spacecraft potential are accurately obtained if the spacecraft is negative, but suffer from errors as the spacecraft potential goes positive and the thin-sheath approximation breaks down.

#### MONOPOLE + DIPOLE MODEL POTENTIAL CONTOURS

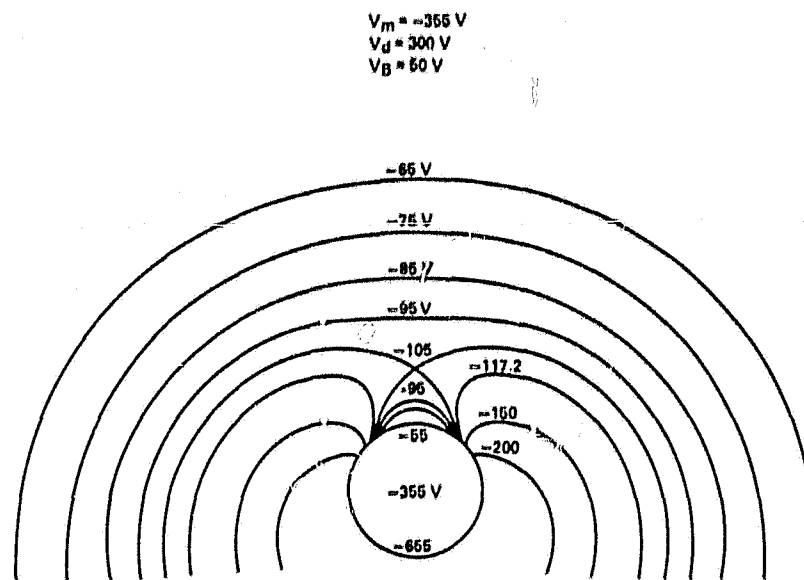


Figure 12. Potential Contours for a Spherical Satellite Geometry with a Differential Potential Across the Spacecraft

Analysis at the University of Alabama in Huntsville of the plasma data obtained on the geosynchronous, three-axis-stabilized ATS-6 satellite showed that in the plasma sheet the mainframe could charge from -10 to -20 kV in eclipse, and -100 V to -2 kV in sunlight. Also, barriers to electron fluxes were observed up to energies of 1 keV. Simple spherical models, such as that in Figure 12, showed that a differential potential across the spacecraft body could produce the observed barrier effects. Application of the NASA Charging Analyzer Program (NASCAP) showed that on ATS-6 the large dish antenna was probably charging 100's to 1000's of volts negative with respect to the mainframe (Olsen, et al., 1981). Operation of the ion engine on ATS-6 as a thruster or a simple plasma emitter was found to be an effective means of reducing or eliminating differential potentials and holding the mainframe near the ambient plasma potential (within a few volts).

Analysis of plasma data from ISEE-1 and SCATHA outside the plasmasphere shows an effect due to azimuthal asymmetries in the spacecraft surface. Both spacecraft show a potential modulation of a few volts with the spacecraft spin period. This is attributed to variations in the photoemission yield of the different materials around the spacecraft circumference. The net photoelectric current varies with the spacecraft rotation, causing the modulation in potential. This is clearly not a differential charging effect, since it is seen on both the insulating SCATHA spacecraft and the conductively coated ISEE-1 spacecraft. Continued studies involving four different spacecraft configurations in the charging plasma conditions of the Earth's magnetosphere will strongly enhance understanding of spacecraft plasma interactive effects. (C. Baugher/ES53/205-453-0029).

Singh, N. and Baugher, C. R.: Sheath Effects on Current Collection by Particle Detectors with Narrow Acceptance Angles. Journal of Scientific Instrumentation (in press).

Comfort, R. H., Baugher, C. R., and Chappell, C. R.: Use of the Thin Sheath Approximation for Obtaining Ion Temperatures from the ISEE-1 Limited Aperture RPA. To be submitted to J. Geophys. Res., 1981.

Olsen, R. C., McIlwain, C. E., and Whipple, E. C.: Observations of Differential Charging Effects on ATS-6. J. Geophys. Res., 86, pp. 6809-6819, 1981.

Olsen, R. C.: Modification of Spacecraft Potentials by Plasma Emission. Journal of Spacecraft and Rockets, September/October 1981.

### Plasma Flow Studies

Because the unique diagnostic requirements of plasma flow interaction studies were not met by existing techniques, a new instrument, the Differential Ion Flux Probe (DIFP), was developed. This unique instrument measures the direction, energy, and flux intensity of multiple ion streams at a single point in space and has subsequently added a substantial new insight into laboratory plasma flow dynamics. In the past year, the DIFP was modified to provide a greater effective aperture area (to achieve higher sensitivity) and developed for flight on the Multiple Auroral Probe (MAP) sounding rocket mission with Southwest Research Institute, where it will measure ion drifts within auroral arcs and explore ion-neutral interactions. A similar instrument, combined with a planar Retarding Potential Analyzer, was delivered to the University of Iowa to be flown on the STS-3 and Spacelab 2 Plasma Diagnostic Package (PDP) experiments, where it will measure ion drifts associated with orbiter-generated ionospheric disturbances (see Figure 13). In addition, the DIFP ion deflection system is the first stage of a swept angle retarding ion mass spectrometer instrument which was tested on a University of Michigan rocket and has been proposed for the Origin of Plasmas in the Earth's Neighborhood (OPEN) mission and for future planetary missions. It is anticipated that more advanced versions of the DIFP will form an important part of the scientific payload of future MAP sounding rocket and Shuttle/Spacelab missions.

ORIGINAL PAGE  
BLACK AND WHITE PHOTOGRAPH

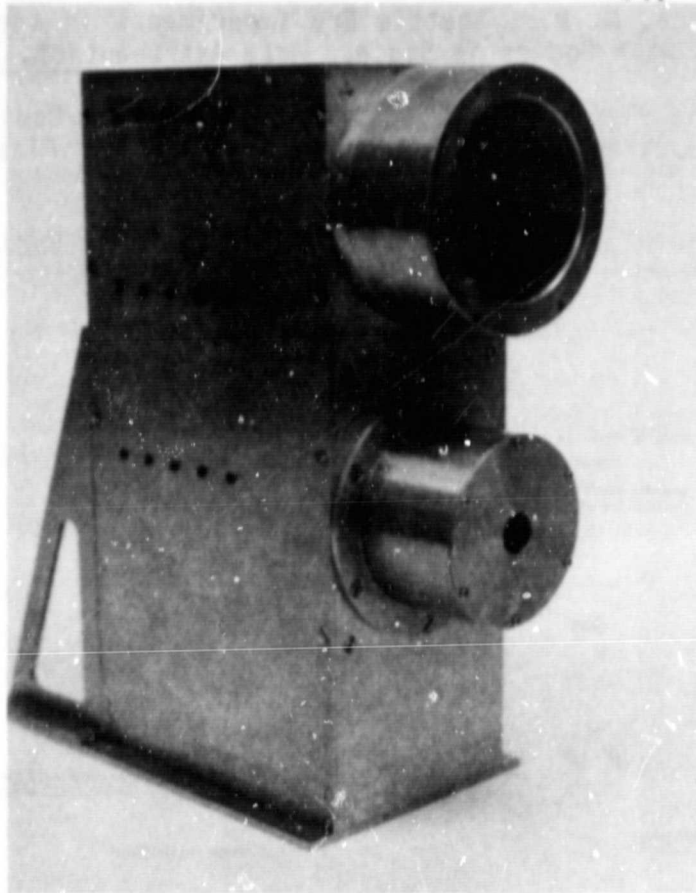


Figure 13. Differential Ion Flux Probe

It has been found that the same methods and techniques developed in the laboratory can be applied to orbital experiments that use the Shuttle and its associated hardware to simulate certain classes of natural plasma flow interactions that are prominent phenomena in the solar system. The interaction occurring between Jupiter's magnetospheric plasma and its moon, Io, is but one of a number of examples. The role of the Shuttle orbital simulation experiments in supplementing and expanding the data from planetary probes has been investigated and is expected to be very similar to that of the laboratory studies in understanding the satellite-ionospheric interaction. Figure 14 shows how such experiments might be conducted, using the Shuttle Orbiter, a tethered test body and diagnostic package, and a maneuverable diagnostic package mapping the regions of disturbed plasma created by the test body. The PDP experiments on the STS-3 and Spacelab 2 missions are the first steps toward this type investigation (N. Stone/ES53/205-4530028).

Stone, N. H.: The Aerodynamics of Bodies in a Rarefied Ionized Gas with Applications to Spacecraft Environmental Dynamics. Ph.D. Dissertation, The University of Alabama in Huntsville (May 1979); also NASA TP (in press).



ORIGINAL PAGE  
BLACK AND WHITE PHOTOGRAPH

Samir, U. and Stone, N. N.: Shuttle Era Experiments in the Area of Plasma Flow Interactions with Bodies in Space. Acta Astronautica, 7, 1091, 1980.

Stone, N. H.: The Plasma Wake of Mesosonic Conducting Bodies, Part 1: An Experimental Parametric Study of Ion Focusing by the Plasma Sheath. J. Plas. Phys., 25, 351, 1981.

Stone, N. H.: The Plasma Wake of Mesosonic Conducting Bodies, Part 2: An Experimental Parametric Study of the Mid-Wake Ion Density Peak. J. Plas. Phys. (in press).

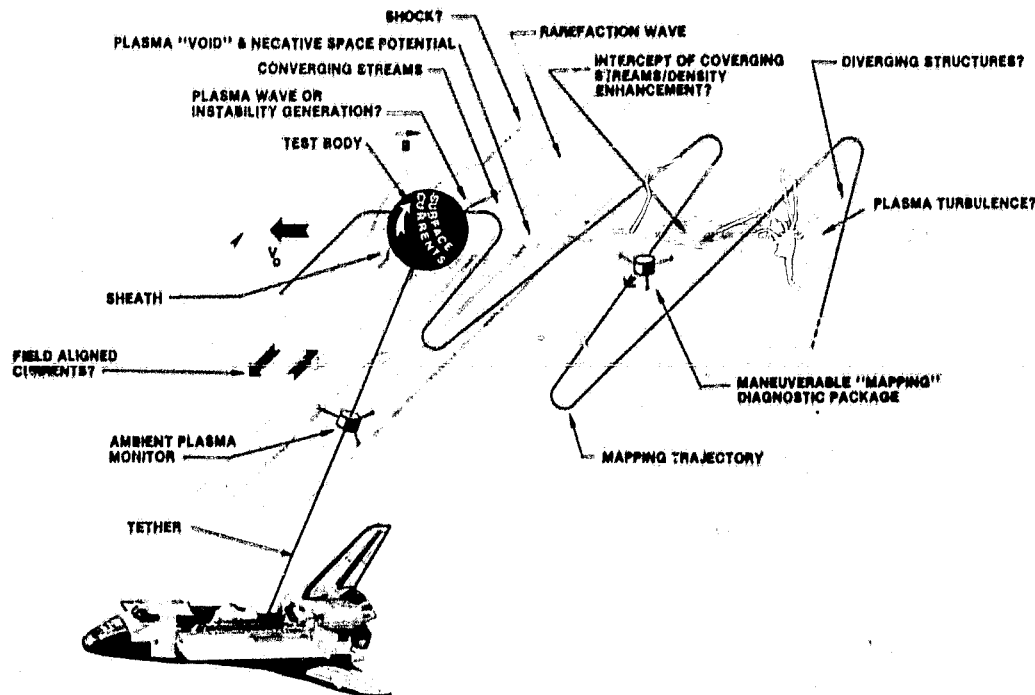


Figure 14. Use of a Tethered Test Body to Conduct Plasma Experiments

Optical Observations of Magnetosphere/Atmosphere Coupling

The primary focus of this activity this past year has been on the development of instrumentation to measure optical signatures originating from the lower thermosphere. These signatures show the processes by which the magnetosphere can drive the Earth's neutral atmosphere and vice versa. A large-aperture Fabry-Perot interferometer has been upgraded to make Doppler measurements of thermospheric winds. This instrument will be operated at the Geophysical Institute, University of Alaska, during Fall 1981/Winter 1982 observing season. Development of image plane detection of faint source emissions for the Fabry-Perot and the Atmospheric Emissions Photometric Imager (AEPI) is also in progress.

ORIGINAL PAGE  
BLACK AND WHITE PHOTOGRAPH

Development of a large-aperture Fabry-Perot interferometer began this year. This instrument was designed to help understand the thermal and dynamic behavior of the upper atmosphere in and near auroral precipitating particle regions. The interferometer (Figure 15) is equipped with a microprocessor-based control system and closed pressure scan system which allows rapid tuning of the instrument's frequency scanning and viewing direction through stepper controlled mirrors. The microprocessor also enables the system to log data and to be controlled by remote users through modem access.

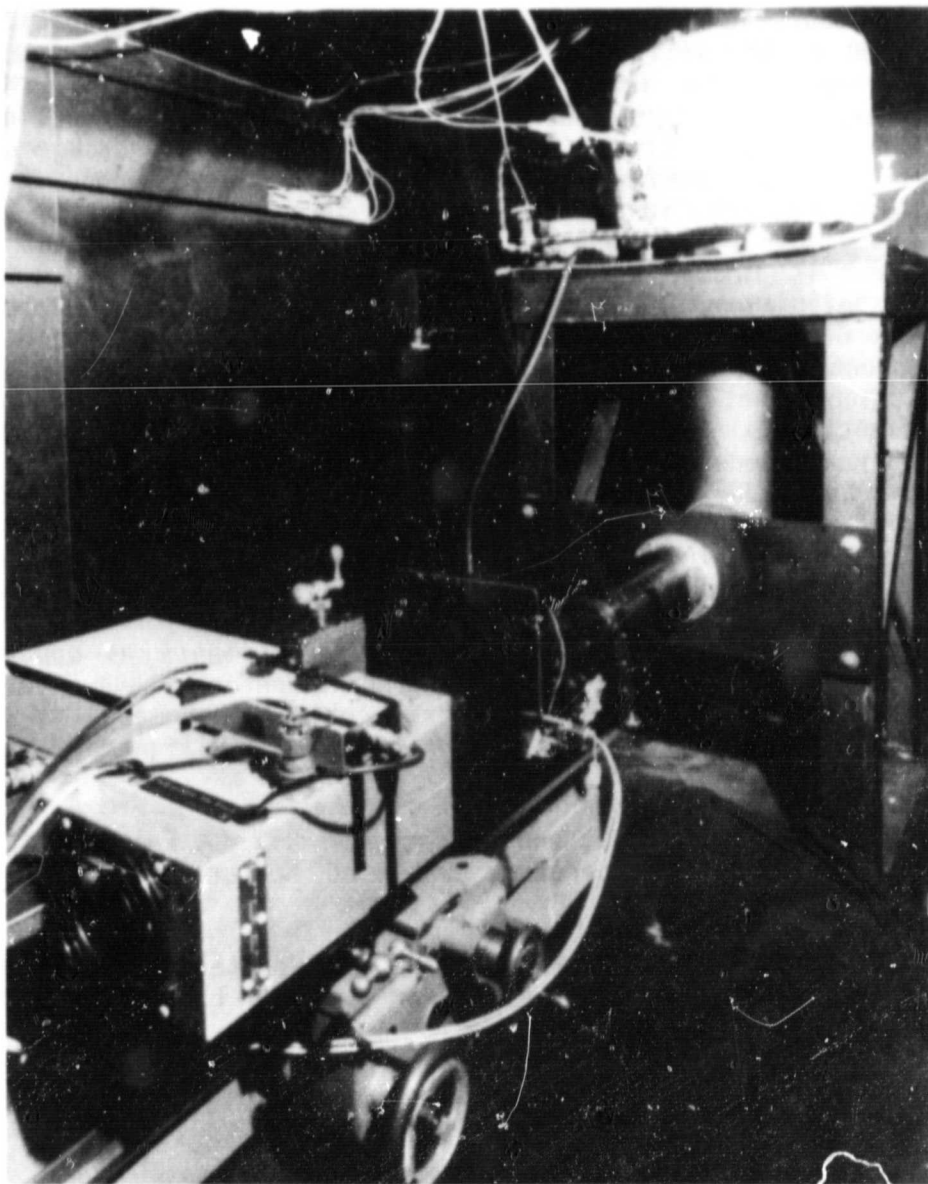


Figure 15. Fabry-Perot Optical and Detection Assemblies

A productive observing season is anticipated in operating the instruments with colleagues at University of Alaska. Several other observing groups in the Northern Hemisphere will also be making simultaneous measurements which will contribute significant new knowledge on thermospheric dynamics responses to auroral precipitation and related effects.

Preliminary design has been completed on the incorporation of a CCD imager (intensified and cooled) into the detection plane of the Fabry-Perot instrument. A 25 mm image intensifier with  $> 500,000$  gain is being assembled and integrated through a 25 to 14 mm fiber optic reducing plug. A CCD array (480 x 388) will be coupled to the device optics and the entire assembly refrigerated for integrating low light level sources. The imager addition is expected to extend the instrument sensitivity several orders of magnitude, allowing simultaneous sensing of line shape and background emission intensities and extending measurements to non-Gaussian line shapes.

The Atmospheric Emissions Photometric Imager (AEPI) is being developed to fly on Spacelab 1 and future Spacelab missions. The instrument has been fabricated and is in the environmental testing stage in preparation for Spacelab 1. Definition of a new image detector for AEPI and related spacecraft imagers has been initiated. This instrument task is oriented toward the development of spacecraft instrumentation for the imaging of faint source emissions that originate in our magnetospheric environment from natural and artificial stimuli. The imager must have a large dynamic range for high contrast scenes such as those produced by auroral beams. Near UV, visible, and near IR wavelength regimes all have emission features of scientific interest.

The imager engineering model being developed will be suitable for ground and balloon-borne experiment applications. The imager will be used in tests with SEC cameras on natural auroral observations for performance evaluation as well as with artificial chemical release experiments as opportunities become available. This development work will, therefore, have direct application to the observation of magnetospheric optical phenomena and will form a strong base of knowledge from which future Spacelab flight systems can be evolved. (G. Swenson/ES53/205-453-3040)

Sivjee, G. G., Hallinan, T. J., and Swenson, G. R.: A Fabry-Perot Imaging System for Thermospheric Temperature and Wind Measurements. J. Applied Optics, 19, p. 2206, 1980.

Sandie, W. G., Mende, S. B., Swenson, G. R., and Polites, M. E.: Atmospheric Emissions Photometric Imaging (AEPI) for Spacelab 1. SPIE Symposium, Los Angeles, February 9-13, 1981.

## Planetary Plasma Processes

### Jupiter

For nearly three decades, intense and variable decametric radio emissions from Jupiter have been observed from the Earth over the frequency range 5 MHz to 40 MHz. Near-Earth satellites have extended the low frequency limit set by the terrestrial ionosphere down to a frequency of 425 kHz. The radiation is characterized by a high degree of elliptical polarization, complex dynamic spectra, and an upper cutoff frequency of approximately 39.5 MHz. Its probability of occurrence, dynamic spectral characteristics, polarization, and intensity are related to the central meridian longitude of Jupiter and to the orbital phase of Io.

Recently the Planetary Radio Astronomy Experiment (PRA) on the Voyager 1 and 2 spacecraft obtained dramatic new information about Jupiter both because of its proximity to Jupiter and because it was able to measure the radio emissions to much lower frequencies than has been possible from Earth and near-Earth observations. A typical frequency-time spectrogram from the Voyager PRA experiment is shown in Figure 16. The figure shows the Jovian dynamic spectrum from 1.2 kHz to 40 MHz over an 8-hour interval. It reveals both the newly discovered nested family of arcs in the decametric spectral region and strong kilometric/hectometric emissions. These emissions are too complex to be explained by simple geometric models.

To understand the generation mechanisms and source locations of the Jovian emissions, a full three-dimensional ray tracing program has recently been developed at MSFC. Incorporated in the MSFC ray tracing program are models of the complex magnetic field and thermal plasma distributions (including the recently discovered Io plasma torus) found in Jupiter's magnetosphere.

The development and testing of the three-dimensional ray tracing program have been completed, and actual calculation of representative ray paths has begun. The validity of these calculated ray paths will be compared with the data accumulated by the PRA experiments on Voyagers 1 and 2 (J. L. Green/ES53/205-453-0028).

Warwick, J. W., et al.: Voyager 1 Planetary Radio Astronomy Observations Near Jupiter. Science, 204,995-998 (1979).

ORIGINAL PAGE  
BLACK AND WHITE PHOTOGRAPH

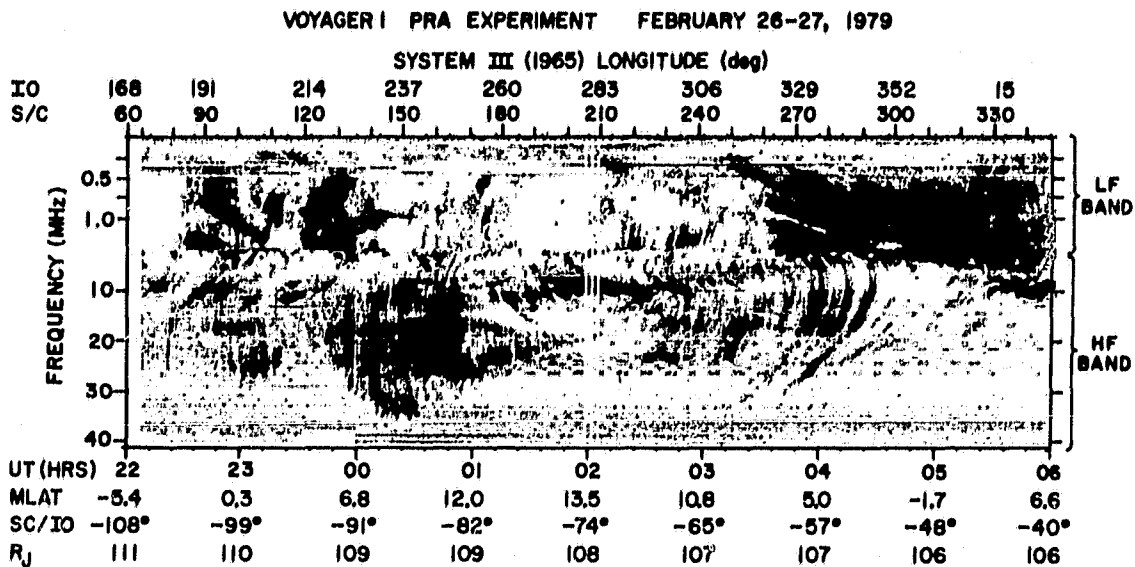


Figure 16. Voyager Observations of Natural Radio Emissions from the Jovian magnetosphere (from Warwick, et al., 1979)

### Saturn

A one-dimensional theoretical model of the Saturn upper atmosphere and ionosphere has been developed at MSFC. This model is composed of a neutral atmosphere code, an ionosphere code, a two-stream electron transport code, and an ion and electron temperature code. All components of the model are coupled together to provide a self-consistent solution of the structure, composition, and temperature of the upper atmosphere and ionosphere of Saturn.

Recent studies using the model have examined the ionosphere in light of recent Voyager 1 measurements of the Saturn atmosphere and ionosphere. This modeling indicates the measured peak electron density of  $2 \times 10^4 \text{ cm}^{-3}$  is an order of magnitude smaller than that expected from modeling results (Figure 17). This discrepancy suggests dynamical or chemical processes affecting the Saturnian ionosphere which are not yet completely understood. Modeling efforts will continue over the next year as the complete Voyager 1 and 2 Saturn encounter data sets are analyzed.

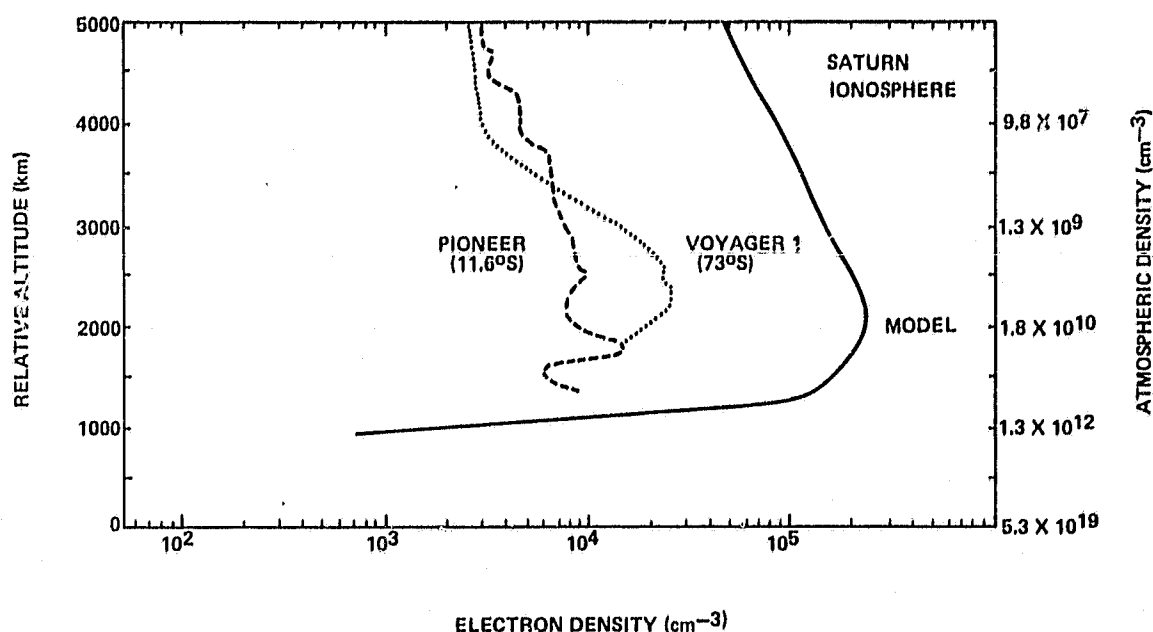


Figure 17. Electron Densities in the Ionosphere of Saturn obtained from Model Calculations and the Pioneer and Voyager Spacecraft

Recent Voyager/Jupiter UVS measurements of  $\text{H}_2$  auroral emissions indicate that approximately  $8 \text{ ergs cm}^{-2}\text{s}^{-1}$  of energetic particle energy is deposited in the Jovian atmosphere in a latitudinal band near  $+65^\circ$  latitude. The energetic particle fluxes appear to originate from wave-particle interactions in the Io plasma torus and may be composed of electrons, protons, or heavier ions such as  $\text{S}^+$  or  $\text{O}^+$ . These particles penetrate the Jovian atmosphere and dissociate and ionize  $\text{H}_2$  as well as heat the atmosphere. This source of atomic hydrogen ( $\text{H}$ ) and heat is believed to be an important contribution to the global energetics and composition of the Jovian upper atmosphere.

The model has been modified to examine the fate of energy cascade processes in the case of Jovian electron aurorae. The results indicate that auroral precipitation processes are important in determining the global distribution of atomic hydrogen in the upper atmosphere of Jupiter and are strong local sources of heating which may have significant effects on the Jovian global circulation. (J. H. Waite, Jr./ES53/0028)

Atreya, S. K. and Waite, J. H., Jr.,: Saturn Ionosphere Theoretical Interpretations. Nature, 1981.

Kliore, A. J., Patel, I. R., et al.: Structure of the Ionosphere and Atmosphere of Saturn from Pioneer 11, Saturn Radio Occultation. J. Geophys. Res., 85, 5857, 1980.

Waite, J. H., Jr., Atreya, S. K., et al.: The Upper Atmosphere and Ionosphere of Saturn. IGA Abstracts and Programme, Proceedings of the 4th IGA Scientific Assembly, Edinburgh, p. 470, 1981a.

Waite, J. H., Jr., Cravens, T. E., et al.: Jovian Electron Aurorae. To be submitted to J. Geophys. Res., 1981b.

## ASTRONOMY

### Optical Astronomy

MSFC's program of ground-based astronomy in 1981 used the f/4 Echelle Spectrograph for observing diffuse astronomical objects. This program studied the HII regions in the galactic spiral arms. Observations of radiation emitted by regions of hydrogen provide information on the physical state in these important regions of star formation. The objects investigated were NGC 7000, NGC 1499, IC 1318, and M16. Detailed modeling of these regions was performed. Also, participation with the French on the Spacelab 1 Very Wide Field Camera experiment continued. This experiment will make an ultraviolet survey from space of large and very faint HII regions and young stars. (G. A. Gary/ES62/205-453-5133)

Mufson, S. L., Fountain, W. F., et al.: An Investigation of the Neutral and Ionized Gas in M16. The Astrophysical Journal. September 1981.

### X-Ray Astronomy

The research program in X-ray astronomy has concentrated heavily on the analysis and interpretation of data from the time interval processor of the Monitor Proportional Counter aboard the HEAO-2 spacecraft. Several extremely interesting objects have been obtained and published in open literature. Of particular interest has been the discovery of a time varying period of the X-ray source Cygnus X-3 and the consequence that the companion to the

X-ray source may be a helium star. Another result of this work led to the pulsed period of the binary source 4U1626-67 and the discovery of time variable fluctuations in the pulse profile.

Significant accomplishments have also been achieved in support of the Advanced X-Ray Astrophysical Facility. Specifically, detailed measurements of the X-ray scattering from a variety of reflecting surfaces using the MSFC X-ray test facility have been accomplished. These are the first such data obtained with sub-arc-second angular resolution and, as such, represent a unique data base for understanding X-ray scattering and relating it to other physical properties of the surface structure. A major result, accomplished as part of this program, was the demonstration of the feasibility of multi-layered, coated optics as a viable tool for accomplishing low energy, narrow band-width, normal incidence X-ray optics. (M. C. Weisskopf/ES62/205-453-5233)

Elsner, R. F., Ghosh, P., Darbro, W., Weisskopf, M. C., Sutherland, P. G., and Grindlay, J. E.: Observations of Cygnus X-3 with the Einstein (HEAO-2) X-Ray Observatory: The Period Derivative and the Asymmetric X-Ray Light Curve. The Astrophysical Journal, 239, 1980, 335-344.

Ghosh, P., Elsner, R. F., Weisskopf, M. C., and Sutherland, P. G.: The Asymmetric 4.8 Hour X-Ray Modulation of Cygnus X-3: Model Light Curves and Inferred Orbital Parameters. The Astrophysical Journal, accepted for publication, December 1980 issue.

### Gamma-Ray Astronomy

On October 6, 1980, a MSFC gamma-ray astronomy experiment was launched on a balloon from the National Scientific Balloon Facility, Palestine, Texas. The large-area detector array performed a variety of high-energy astronomy observations and served as a test of detector components for the planned Gamma-Ray Observatory mission. This balloon experiment and the JACEE experiment, described elsewhere in this document, passed almost directly over Huntsville, Alabama, where a down-wind telemetry station had been set up (Figure 18). More than 26 hours of useful data were recorded before the experiment hardware landed near Roanoke, Virginia. It was recovered in good condition for future use.

Preliminary data analysis has uncovered some interesting results. A gamma-ray burst, the primary objective of the experiment, has been detected and measured more accurately than that from any previous balloon experiment. The burst, which lasted approximately 15 sec, covered a wide energy range and was observed to fluctuate on time scales as short as 1/10 sec. Current theories suggest that a burst is the result of a large thermonuclear explosion on the surface of a neutron star. X-rays from two weak solar flares were also detected by the MSFC experiment and were confirmed by other spacecraft in Earth orbit. These served as useful calibration events for the experiment. Pulsing, hard X-rays were detected from the pulsar in the



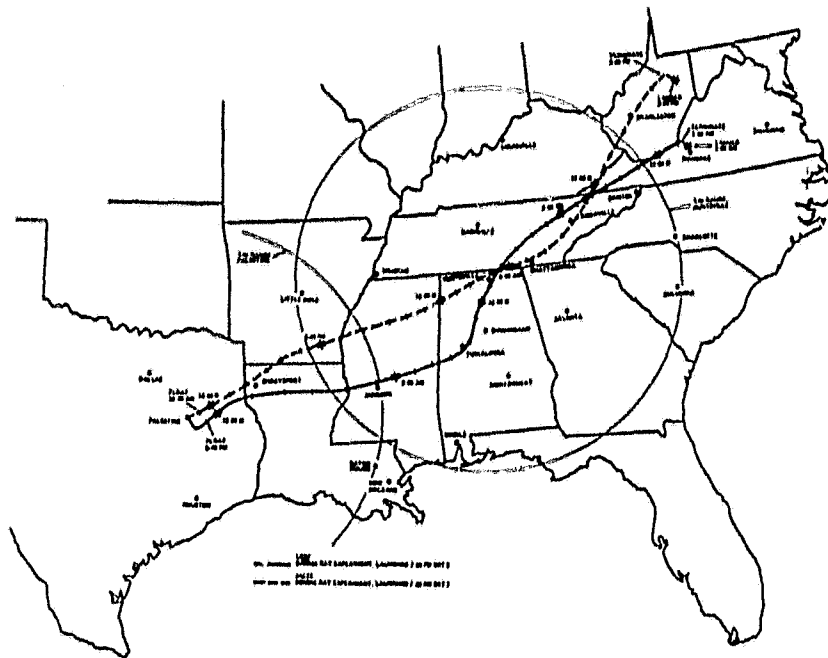


Figure 18. Trajectories of the Two Balloons Launched on October 6 - 7, 1980. (Tick Marks Indicate One-Hour Intervals)

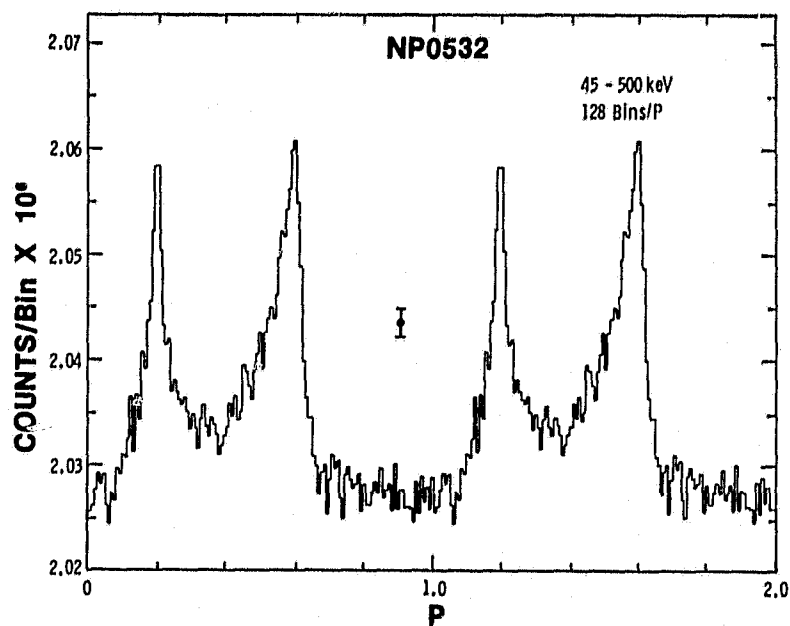


Figure 19. Pulse Profile from The Crab Nebula, NP0532, from the October Balloon Flight

Crab Nebula (NP0532) and from a transient binary source, A0535+26. These observations, which will soon be published, are the most sensitive observations of these two objects in this energy range (Figure 19). (G. Fishman/ES62/205-453-0117)

Wilson, R. B., Fishman, G. J., and Meegan, C. A.: Observation of a Gamma-Ray Burst and Other Sources with a Large-Area, Balloon-Borne Detector. Workshop on Gamma-Ray Transients and Related Astrophysical Phenomena, La Jolla, California, August 5-8, 1981; to be published in Conference Proceedings, AIP, 1981.

Fishman, G. J., Meegan, C. A., Parnell, T. A., and Wilson, R. B.: The Burst and Transient Source Experiment for the Gamma-Ray Observatory. Workshop on Gamma-Ray Transients and Related Astrophysical Phenomena, La Jolla, California, August 5-8, 1981; to be published in Conference Proceedings, AIP, 1981.

### Cosmic-Ray Research

For the past several years, MSFC has been involved in a series of experiments to investigate the composition and energy spectra of cosmic rays above  $10^{12}$  electron volts (1 TeV). Previously, only large assemblies of detectors on the ground (air shower arrays) and one satellite experiment launched by the USSR had reported energy and composition data in this energy range--with many incompatible results.

The MSFC effort is part of a collaboration with investigators from several United States and Japanese universities and institutions and is called the Japanese American Cooperative Emulsion Experiments (JACEE). The core instrument is a large stack of nuclear track "photographic" emulsions, etchable plastics, various X-ray films and lead plates called an "emulsion chamber." The cosmic-ray nuclei and their interaction products leave microscopic tracks that are analyzed after the flight to determine the energy and identity of the primary cosmic ray, and the characteristics of nucleus-nucleus interactions at extreme energies. MSFC has been involved in three such experiments, starting in 1979, and has developed the instrumentation and performed balloon flights of the large balloon-borne experiments.

New results concerning the composition of cosmic rays above  $10^{12}$  electron volts have resulted from an October 1980 balloon flight. Nuclei of hydrogen (protons) and helium (alpha particles) have been measured to  $10^{14}$  and  $10^{13}$  electron volts, respectively, and show spectra similar to that below these energies--which are at variance with some earlier results.

The heavier nuclei from lithium through iron may become relatively more abundant at energies above  $10^{14}$  electron volts--a surprising result but one in keeping with many air shower array measurements. Many heavy nucleus-nucleus collisions and their secondary products have been examined to search for evidence of nuclear material shock waves and "super dense" nuclear matter.

Figure 20 shows the electronic instruments developed at MSFC being prepared for the JACEE 3 balloon flight. These detectors (Cerenkov counters and multiwire proportional counters) are used to measure definitively the

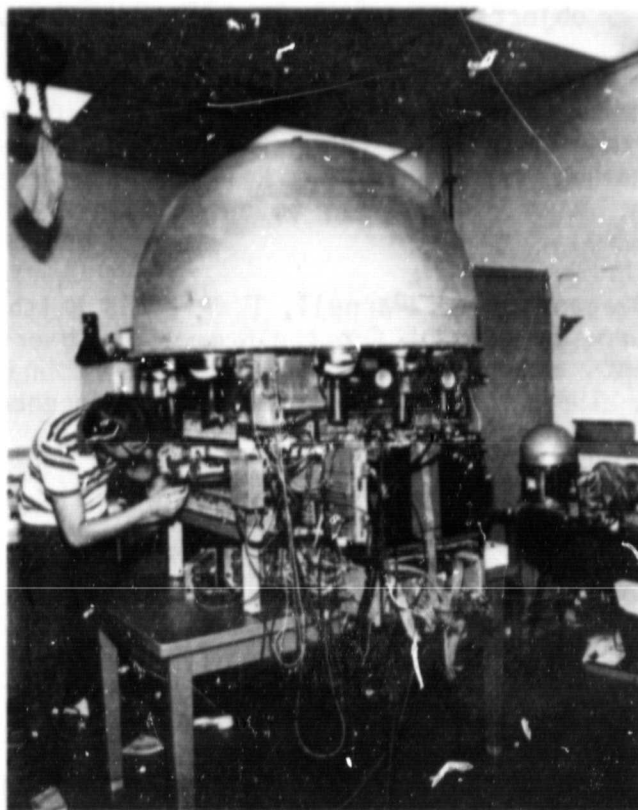


Figure 20. Cosmic-Ray Instruments Being Prepared for the October 1980 Balloon Flight

nuclear species and energy of the cosmic rays up to 5 TeV total energy. The cosmic rays which go through these counters will undergo catastrophic nuclear interactions in an emulsion chamber below the counters. The counters will characterize the incident cosmic-ray beam. (T. Parnell/ES62/205-453-5133)

Gregory, J. C., Parnell, T. A., et al.: Proton Spectrum in Energy Range  $10^{12}$  -  $10^{14}$  eV. 17th International Cosmic Ray Conference, Paris, July 1981, Conference Papers, Vol. 1, 1981, p. 107.

Ogata, T., Parnell T. A., et al.: Chemical Composition of Cosmic Rays at Energies Greater than  $10^{13}$  eV. 17th International Cosmic Ray Conference, Paris, July 1981, Conference Papers, Vol. 2, 1981, p. 119.

Ogata, T., Parnell, T. A., et al.: Heavy Ion Collisions at Energies Greater than 100 GeV/n. 17th International Cosmic Ray Conference, Paris, July 1981, Conference Papers, Vol. 5, 1981, p. 85.

Burnett, T. H., Parnell, T. A., et al.: Proton-Nucleus Interactions at Energies around 100 TeV. 17th International Cosmic Ray Conference, Paris, July 1981, Conference Papers, Vol. 5, 1981, p. 125.

Gregory, J. C., Watts, J. W., Parnell, T. A., et al.: A Measurement of the Response of Xenon-Filled Ion Chambers to Cosmic Ray Nuclei above 20 BeV/Nucleon. 17th International Cosmic Ray Conference, Paris, July 1981, Conference Papers, Vol. 8., 1981, p. 48.

Huggett, R. W., Parnell, T. A., et al.: Japanese-American Cooperative Emulsion Experiment (JACEE). 17th International Cosmic Ray Conference, Paris, July 1981, Conference Papers, Vol. 8, 1981, pp. 80-87.

### ATMOSPHERIC SCIENCES

The objective of research activities in the atmospheric sciences is an improved understanding of atmospherical processes. Studies involve satellite sensor system definitions, utilization of data acquired through correlative field experiments and laboratory research, development of Shuttle/Spacelab experiments, and the acquisition of new knowledge on the thermodynamic and kinematic properties of the atmosphere.

#### Sensor Evaluation and Mesoscale Sampling Program

Two main efforts have been carried out in this program at MSFC. The first was the experiment design and field readiness tests for the 1982 VISSR Atmospheric Sounder (VAS) evaluation and representativeness experiment. This experiment, originally scheduled for March 1981, was delayed due to sensor availability restrictions on GOES D. It will be run in the Spring of 1982 using GOES E. A limited version was carried out in Montana in July 1981 during four VAS/CCOPE (Cooperative Convective Precipitation Experiment) days. These tests used rawinsonde units furnished by MSFC to collect upper-level data. Data from this experiment will be used to evaluate VAS capabilities under marginal viewing angle conditions and weak gradients of meteorological parameters. The second main effort was a study of the tracking precision of the rawinsonde system used in mesoscale and ground truth experiments. The purpose of this effort was to provide a benchmark for the accuracies of wind and thermodynamic measurements obtained from the primary system used to provide upper-level data in evaluation programs for satellite-derived winds and temperature/moisture fields. Results from these field evaluation programs will significantly improve the understanding of how satellite sensors depict the atmosphere. They will also permit an understanding of restrictions which must be placed on the use of satellite data as the scales studied become smaller in space and time compared to conventional synoptic scales. (J. Arnold/ES84/205-453-4175)

## Mesoscale Research

The research portion of the mesoscale program is carried out using special space and conventional observations acquired by MSFC for selected storm periods. Specific research efforts include: (1) automated mesoscale winds determined from GOES satellite imagery, (2) storm environment interactions determined from Atmospheric Variability Experiment (AVE)-SESAME and satellite data, (3) diagnostics of severe convection and subsynoptic-scale ageostrophic circulations, (4) an application of VAS/TIROS sounding information to define vertical circulation in potential storm areas, (5) storm environment energetics, (6) mesoscale circulations and convective storm formation, (7) the moisture budget of the severe storm environment as determined from AVE and satellite data, and (8) a study of the application of the MSFC Doppler Lidar to research on mesoscale atmospheric phenomena. The MSFC portion of these research programs has been greatly enhanced by the upgrading of hardware and software of the Mesoscale and Severe Storms computer system and the addition of an image processing and data handling Man-Computer Interactive Data Access System (McIDAS).

MSFC, through the mesoscale program, has made several important contributions in technology development and predictive capability for mesoscale atmospheric phenomena. These include the medium-range thunderstorm forecasts from the limited area, fine mesh being tested at the National Severe Storms Forecast Center and at the Air Force Severe Weather Forecast Section, and a program directed at implementing automated cloud winds using computer tracking of cloud vectors in the operational mode through testing in the McIDAS environment. (G. Wilson/ES84/205-453-2570)

Wilson, G. S., and Turner, R. E.: Objective Predictions of Thunderstorm Location and Severity for Aviation. Journal of Aircraft, accepted for publication.

## Ionosphere-Severe Storms Coupling

Investigations of gravity waves observed with a ground-based Continuous Wave High Frequency (CVHF) Doppler array during the past few years have shown that those waves with periods from 10-15 and 20-30 min and wavelengths of 100-150 km are associated with and generated by the weather systems that produce tornadoes approximately 1 to 2 hours after the waves are initiated. Preliminary analyses this year of the GOES visible and IR imagery of clouds that produced tornadoes indicate that the following criteria are required for tornado development: (1) Convective overshooting turrets with tops significantly above the tropopause; (2) a critical growth rate of these turrets (not yet determined); (3) the critical volume and mass of the turret; and (4) the tornadoes touch down between 15 and 30 minutes after the convective turrets exceed both the critical growth rates and critical volume/mass, when the satellite imagery show rapid collapsing of the turrets. Additional storms are being investigated to determine the absolute values of the critical parameters with a view toward developing a fully automated, on-board system for a geostationary satellite. (R. E. Smith/ES81/205-453-3101)

## Lightning Research

As part of the Lightning Mapper Sensor development program at MSFC, a series of research activities is being pursued. These research efforts are focused on developing a quantitative data base required for the design of an optical lightning sensor.

A primary research activity involves measurements of lightning characteristics from above thunderstorms using a NASA U-2 aircraft. Four new optical instruments were developed and installed aboard the U-2 during 1981 in order to enhance existing capabilities. Five flights were made over active thunderstorms in the southwestern United States during the summer of 1981 with the expanded instrument package. These flights, which were conducted under both daytime and nighttime conditions, have generated a unique data set that includes cloud background brightness and the optical amplitude and duration of individual lightning strokes at specific emission wavelengths.

The U-2 flights also serve to generate reference measurements which will be used in the interpretation of data that will be obtained with the Nighttime Daytime Optical Survey of Lightning (NOSL) experiment scheduled for flight on STS-2. All NOSL hardware was completed and shipped to Kennedy Space Center for integration into the Shuttle during 1981.

Ground-based observations of lightning were also made as a complement to the airborne effort. High-quality spectra from more than 150 lightning flashes were obtained. The data include not only ground strokes but also a number of air discharges and step leaders. This data set represents a significant improvement over previous work. The spectral range covered includes the visible and the very important near infrared. (H. Christian/ES83/205-453-2463)

Christian, H. J., Jr.: Lightning Detection and Location Techniques. AIAA 19th Aerospace Sciences Meeting, January 12-15, 1981.

Vaughan, O. H., Vonnegut, B., Brook, M., and Orville, R. E.: Thunderstorm Overflight Program. Paper 80-1934-CP, Proceedings AIAA Conference on Sensor Systems for the 80's, CP-807, AIAA, New York, 1980.

## Cloud Physics

Research on warm cloud physics is directed toward applying low-gravity methods to the solution of selected problems in the microphysics of the formation and evolution of warm (ice-free) clouds. A theoretical study of cloud droplet growth was completed, and the results have been published. The major elements of the equipment pallet for a KC-135 experimental study of cloud drop growth were assembled and flown, and the concept of the method was successfully verified (Figure 21). After the addition of an aerosol generation system and other instrumentation, the system was flown again in April and May 1981. Good data sets were obtained, and data analysis is in progress. Three other experiments were successfully flown on KC-135 flights to observe properties of ice crystal growth and related cold cloud phenomena as part of a continuing development program in cloud physics. (B. Anderson/ES83/205-453-5219)



Figure 21. Warm Cloud Physics Experiment on the KC-135 Aircraft  
(Front Center Pallet)

Anderson, B. J., Hallett, J., and Beesley, M.: An Extended Classical Solution of the Droplet Growth Problem. NASA TM-82392, January 1981.

#### Global Weather Satellite Studies

The goal of the OSTA Global Weather Program satellite studies at MSFC is to combine the observational capabilities of satellite systems and dynamical knowledge and principles to further understanding and enhance the capability for predicting the structure and evolution of global weather. The studies include (1) oscillations in mid- and high-latitude atmospheric flow (4 to 30 days), (2) the effect of moisture on the broad ascending motion in the cyclonic systems resulting in stable precipitation, and (3) the diagnosis of the energy state and transformation in cyclonic systems, including the parameterization of convection in the storm systems.

Research during the past year yielded a number of significant results. For weak differential solar heating between the equator and the poles, the symmetric circulation appears. As the heating is increased, the flows break down into the wave-like patterns typically observed in mid- and high lati-

tudes with the presence of hysteresis effect depending on the change of wave number from low to high or vice versa. When the nonlinear spectral equations with orographic forcing were integrated, the solution turned out to be doubly periodic, much like the atmospheric index cycle (change from west-east flow to north-south flow and vice versa). The model can switch from a symmetric circulation to a low index blocking pattern at certain critical values of forcing function.

The effect of latent heat release is more subtle. A theoretical study indicates that, when the release of latent heat is introduced in a two-level model, two unstable modes appear. The first mode has a narrow region of strong ascending motion and a wide region of weak descending motion, and the second mode has a narrow region of strong descending motion and a wide region of weak ascending motion. An important case study reveals that the latent heat release has a significant effect on the mean meridional overturnings.

Dutton, J. A.: Fundamental Theorems of Climate Theory -- Some Proved, Some Conjectured. SIAM Review, in press, 1982 publication.

Mitchell, K. E., and Dutton, J. A.: Bifurcations from Stationary to Periodic Solutions in a Low-Order Model of Forced, Dissipative Barotropic Flow. J. Atmos. Sci., 4, 1981, 690-716.

Saltzman, B. and Tang, C-M.: Effects of Variation of Static Stability and Vertical Wind Shear on the Evolution of a Primary Baroclinic Wave. Third Conference on Atmospheric and Oceanic Waves and Stability, AMS, January 19-22, 1981.

Saltzman, B., and Tang, C-M.: A Review of Some Analytical Studies of Finite Amplitude Baroclinic Waves, Including a New Algorithm for the Saturation Effects of Static Stability and Baroclinicity Variations. (Submitted to the Special Centennial Issue of the J. Meteor. Soc. Japan)

Tang, C-M.: The Influence of the Time Change of Static Stability and Wind Shear on Baroclinic Waves. Pure & Applied Geophys. 118, 1980, 706-719.

Tang, C-M.: Physical Mechanism of Baroclinic Waves. Review of Selected Meteorological Topics in Memory of Dr. Grace Zon-hwa Feng Weigel, pp. 15-30, 1981 (in Chinese).

Tang, C-M., and Fichtl, G. H.: The Role of Latent Heat Release in Baroclinic Waves -- Without Beta Effect. J. of the Atmospheric Sciences (submitted).

#### Fifth Annual Workshop on Aviation Meteorology Research

Five aviation meteorological and environmental workshops were held. The major objective of these annual workshops is to provide a consensual view of aviation weather from the users, suppliers, regulators, researchers, and educators. Topics considered by this group deal with the specific aviation weather requirements of the users and regulatory agencies; with the



adequacy of operational procedures, design criteria, safety requirements, and training methods; with status of on-going research programs; and with definition of new programs. This year, the workshop produced sixty-six recommendations, dealing principally with accuracy of weather forecasting, meteorological training, and new equipment. (D. Camp/ES82/205-453-2087)

### Shuttle Turbulence Simulation

A three-dimensional non-recursive model for atmospheric turbulence based on the Von Karman spectrum has been developed this year. This model provides for simulation of instantaneous gusts and gust gradients along the flight path of the Space Shuttle. The model is based on a set of tapes containing a non-dimensional turbulence simulation. The spectral accuracy of these tapes has been demonstrated, guaranteeing the accuracy of any dimensional turbulence generated later. Real-time gust environments for any Shuttle mission can be simulated from an altitude between 120 km and the surface. The ability to simulate turbulence with an a priori guarantee of spectral accuracy from one set of tapes is a marked improvement over currently used models. (W. Campbell/ ES82/205-453-1886)

Tatom, F. B., Fichtl, G. H., Smith, S. R., and Campbell, C. W.: Simulation of Atmospheric Turbulent Gusts and Gust Gradients. Journal of Aircraft (accepted for publication).

Tatom, F. B., and Smith, S. R.: Shuttle Simulation Turbulence Tapes (SSTT) Users Guide. NASA CR-161604, September 1980.

### Design of the Atmospheric General Circulation Experiment (AGCE) for Spacelab Flights

Previous laboratory experimental modeling of large-scale atmospheric flows has been limited to cylindrical geometries. However, in the low-gravity environment of Spacelab, true spherical models can be realized. A radial dielectric body force can be used to simulate gravity, and the complicating effects of terrestrial gravity disappear. Preliminary design feasibility studies indicate that to achieve the required baroclinic instability (wavecyclone instability), a liquid with special properties must be found and the instrument must be carefully designed. Also, techniques for flow and temperature measurement are required. To define the regions of baroclinic instability, basic state and linear stability numerical models are being developed. This work is being performed in conjunction with USRA and Drake University. Other studies to deepen the understanding of the AGCE and to relate the AGCE more closely to atmospheric dynamics research are being performed with the University of Arizona, the University of Miami, and the University of Tennessee Space Institute. These studies also assist in defining scientifically valuable experiments for the AGCE. (W. Fowles/ ES82/205-453-2047)

Geisler, J. E., and Fowlis, W. W.: Theoretical Regime Diagrams for Thermally Driven Flows in a Beta-Plane Channel in the Presence of Variable Gravity. NASA TM-78316, November 1980.

Hyun, J. M.: The Applicability of the Piecewise Linear Current Profile in a Baroclinic Instability Problem. J. of Meteorological Soc. of Japan, 58, No. 6, 1980.

Giere, A. C., and Fowlis, W. W.: Baroclinic Instability with Variable Static Stability--A Design Study for a Spherical Atmospheric Model Experiment. Geophys. and Astrophys. Fluid Dynamics, 16, 1980, 207.

Hyun, J. M.: Separate and Combined Effects of Static Stability and Shear Variation on the Baroclinic Instability of a Two-Layer Current. J. of the Atmospheric Sciences, 38, No. 2, 1981, 322-333.

Antar, B. N., and Fowlis, W. W.: Baroclinic Instability of a Fluid in a Rotating Channel. The 33rd Meeting of APS/Division of Fluid Dynamics, November 1980; abstract: Bull. Amer. Phys. Soc., 25, No. 9, 1980, 1077.

Hyun, J. M., Fowlis, W. W., and Warn-Varnas, A.: Comparison of Numerical Results and Laser Measurements for Stratified Spin-Up Experiments. Third Conference on Atmospheric and Oceanic Waves and Stability, AMS, January 19-22, 1981.

Antar, B. N., and Fowlis, W. W.: Baroclinic Instability of a Real Hadley Cell. Third Conference on Atmospheric and Oceanic Waves and Stability, AMS, January 19-22, 1981.

Giere, A. C., and Fowlis, W. W.: A General Solution of the Eady-Type Equation of Baroclinic Instability. Third Conference on Atmospheric and Oceanic Waves and Stability, AMS, January 19-22, 1981.

Fowlis, W. W.: Results of the Research Program for the Design and Construction of a Spherical Baroclinic Experiment for Spacelab Flights. Third Conference on Atmospheric and Oceanic Waves and Stability, AMS, January 19-22, 1981.

Antar, B. N., and Fowlis, W. W.: Baroclinic Instability of a Real Rotating Hadley Cell. J. of the Atmospheric Sciences, accepted for publication in October 1981 issue.

Giere, A. C., and Fowlis, W. W.: A General Solution of the Eady-Type Equation of Baroclinic Instability. Geophys. and Astrophys. Fluid Dynamics, accepted for publication.

## MATERIALS PROCESSING IN SPACE

The major goal of this program is to stimulate the scientific community to consider space experimentation as a logical extension of on-going terrestrial research when it is desired to investigate or suppress a gravitational effect. At present, approximately 80 research efforts are being sponsored at universities, industries, and other government agencies. This effort has revealed some rather subtle and unexpected effects which will be discussed in subsequent paragraphs.

Another goal of this program is to encourage industry to develop space processing as a commercially viable resource for investigating process control, for producing exemplary materials, and for manufacturing limited quantities of materials with high intrinsic value. This is accomplished by NASA/Industry Joint Endeavor Agreements (JEA), Industrial Guest Investigator (IGI) Agreements, and Industrial Technical Exchange Agreements (TEA). Last year, one JEA was signed and two are now in negotiation; one IGI was signed and another is in negotiation; and three TEA's were signed and two more are under negotiation.

Materials Processing in Space Program Tasks, NASA TM-82443, 1981.

Materials Processing in Space: A survey of Refereed Open Literature Publications, NASA TM-82425, July 1981.

### Crystal Growth

#### Melt Growth

Limits of stability were established for dilute binary systems growing from the melt in a gravitational field in which there exists stabilizing thermal gradients and destabilizing solutal gradients. This occurs in solidification of binary and multicomponent systems in which the rejected solute is less dense than the bulk melt. The surprising result was that such systems become unstable well before density inversion occurs. This is caused by the difference in rates of mass and thermal diffusion. A vertically displaced fluid element will come to thermal equilibrium before it can come to chemical equilibrium; thus it becomes less dense than the surrounding liquid and will continue to rise. These limits are being verified by experiments in model systems using mixtures of succinonitrile and ethanol, which have solidification behavior similar to metallic systems but are transparent and allow a detailed study of the fluid motion in the vicinity of the interface.

Similar stability analyses were initiated for systems in which the rejected component is denser than the bulk fluid. Specifically, such systems may be subject to an over-stability situation, permitting growth rate fluctuations, or may have shape instabilities arising from the more dense rejected component flowing because of gravity to the lowest point on a curved interface. Since an increased concentration of rejected solute lowers the freezing temperature, a slightly curved interface tends to become more curved. Also, any radial thermal gradients, which are unavoidable in Bridgman growth, alters the diffusion profile in the vicinity of the growth interface and further exacerbates the distortion of the growth interface. Flight experiments are being developed in which these gravitational-induced instabilities will be eliminated. The materials chosen are PbSnTe (rejected component less dense than bulk melt) and HgCdTe (rejected component more dense than bulk melt). These systems represent extreme examples of the instabilities discussed and also have significant military and industrial importance as infrared detector materials. (R. J. Naumann/ES71/205-453-0940)

### Vapor Transport

Detailed numerical modeling of the vapor transport in closed ampoules was carried out. It was shown that diffusion fluxes, through viscous interactions with the wall, establish density gradients which are convectively destabilizing even in configurations which, classically, were considered convection-free (i.e., vertical tube heated from the top). It was demonstrated that the vapor transport growth in a gravity field is much more complicated than previously realized and that diffusion-controlled conditions in low-g cannot be approximated by extrapolating from low-pressure systems in unit-g or by growth in a vertical, thermally stable configuration. This probably explains the anomalous transport rates observed on Skylab and ASTP vapor crystal growth experiments. These studies support planned experiments in vapor growth of HgCdTe and CuInS<sub>2</sub>, which have technological importance as infrared detectors, and HgT<sub>2</sub> which is an important gamma-ray energy dispersive analyzer. (R. J. Naumann/ES71/205-453-0940)

### Solution Growth

Recent X-ray topographs of triglycine sulfate (TGS) crystal grown by the conventional technique, in which forced convection is introduced by stirring, show a large number of microscopic liquid inclusions which are believed to limit the performance of this material as an infrared detector. It is conjectured that such inclusions can be reduced or eliminated by growth in a diffusion-controlled environment which can only be realized in a low-g environment. Models for this process have been developed, and the necessary physical parameters such as diffusion constant, solubilities as a function of temperature, index of refraction of the growth solution as a function of concentration and temperature, thermal conductivities of the crystal and the solution, etc., have been measured. A low-g growth experiment will be carried out on Spacelab 3 in which the growth process will be monitored by holography. This will allow the postflight reconstruction of the thermal and concentration fields and will reveal any effects of low-level accelerations associated with the vehicle. (R. J. Naumann/ES71/205-453-0940)

## Metals, Alloys, and Composites

### Monotectic Alloys

A large number of metallic systems have a liquid phase miscibility gap which prevents the formation of finely dispersed alloys by normal freezing in unit gravity because the density differences between the two liquid phases lead to very rapid sedimentation. Early experiments on such systems in ASTP and on SPAR rockets also resulted in massive phase separations, indicating that mechanisms other than gravity were important in producing such phase separation. A number of experiments have been carried out using transparent model systems such as succinonitrile and water/heavy water. By adjusting the amount of heavy water, the systems can be neutrally buoyant at a particular temperature. With such systems, nucleation and growth of the second phase can be studied in detail, as well as droplet migration by solutal and thermal Marangoni convection, droplet interactions with the solidification front, and capillarity effects from the container wall. A recent SPAR rocket experiment demonstrated that massive phase separation can be avoided in metallic systems by choosing the crucible wall so that it is wetted by the majority phase in preference to the minority phase. (R. J. Naumann/ES71/205-453-0940)

### Eutectic Systems

Recent SPAR experiments revealed that a eutectic composition of MnBi/Bi grows with a closer, more regular spacing of smaller MnBi rods than an identical system grown in a vertical stabilizing configuration on the ground. This is an unexpected result since the classical theory of eutectic growth assumes the process to be completely dominated by diffusion. These effects will be further investigated in ground-based experiments using magnetic fields to suppress convection. (R. J. Naumann/ES71/205-453-0940)

### Casting Experiments

Several casting experiments have been carried out in high-g (using a centrifuge) and in low-g using SPAR rockets and KC-135 aircraft flying parabolic trajectories. The high-g samples showed a very fine, equiaxed grain structure apparently caused by dendrite breakage and convective transport. The low-g samples showed fewer, much larger grains with significantly larger dendrite arm spacings, as was expected from earlier SPAR experiments using transparent model systems. Preliminary work has begun on low-g solidification of cast iron. This work is under a Technical Exchange Agreement with John Deere and Bethlehem Steel in an effort to provide a better understanding of the control of graphite formation and morphology. (R. J. Naumann/ES71/205-453-0940)

## Containerless Processing

### Glass Fining

A glass fining experiment was carried out in a SPAR rocket flight. Samples containing various sized bubbles were melted and subjected to a thermal gradient. Bubble migration due to surface tension-driven convection (Marangoni flow) was observed, although there appears to be some discrepancy between the observed migration and theoretical predictions. However, the possibility of using this technique for fining glasses in low-g has been confirmed. (R. J. Naumann/ES71/205-453-0940)

### Containerless Technology Demonstrations

Several containerless processing technology experiments have been carried out during SPAR flights using a 3-axis acoustic levitator operated in an ambient temperature. Liquid droplets were deployed and captured by the sound field. Oscillation and rotation were demonstrated by modulating the amplitude and phase of the sound field. A bubble was injected into the drop to investigate possible bubble centering mechanisms, including oscillation, rotation, and adiabatic decompression. Droplets of different colored liquid were deployed and merged to study mixing and homogenization in a containerless environment. This effort is partially supported by DOE in conjunction with Lawrence Livermore Labs to investigate the formation of highly concentric fuel containment shells for the inertial-confinement fusion (ICF) program. (R. J. Naumann/ES71/205-453-0940)

### Electrophoresis

An extensive modeling program has been carried out to determine the gravitational influences and limitations of continuous flow electrophoresis. This has been complemented by experiments in carefully designed, well-instrumented flow chambers that allow decoupling of the many complicating gravitational influences. It has been demonstrated that the most sensitive and difficult to control disturbing parameter is the lateral thermal gradient. Lateral gradients as small as  $0.1^\circ\text{K}/\text{cm}$  are sufficient to produce sample stream meandering and loss of resolution in wide-gap machines. This is normally controlled in commercial machines by use of a very narrow flow channel, but at considerable expense in throughput and loss of resolution from wall effects. In addition to establishing a clear rationale for performing electrophoresis in space, this research has led to two concepts in machines for terrestrial use. One concept uses highly conductive, heat-sinked walls to reduce the lateral gradients. Another concept is a novel moving wall approach that allows the use of a narrow gap without introducing sample stream distortions. Preliminary tests of these concepts are encouraging. Also, these concepts could be employed in low-g with even greater performance possibilities and thus form the basis for the next generation of space electrophoresis devices. (R. S. Snyder/ES73/205-453-3537)

ORIGINAL PAGE IS  
OF POOR QUALITY

## SYSTEMS DEFINITION

MSFC has a number of studies underway of future projects and payloads which serve as a focus for the R&T projects. At the same time, these studies also identify desirable missions that may be contemplated for the Agency.

### GROUND LAUNCHED TRANSPORTATION SYSTEMS

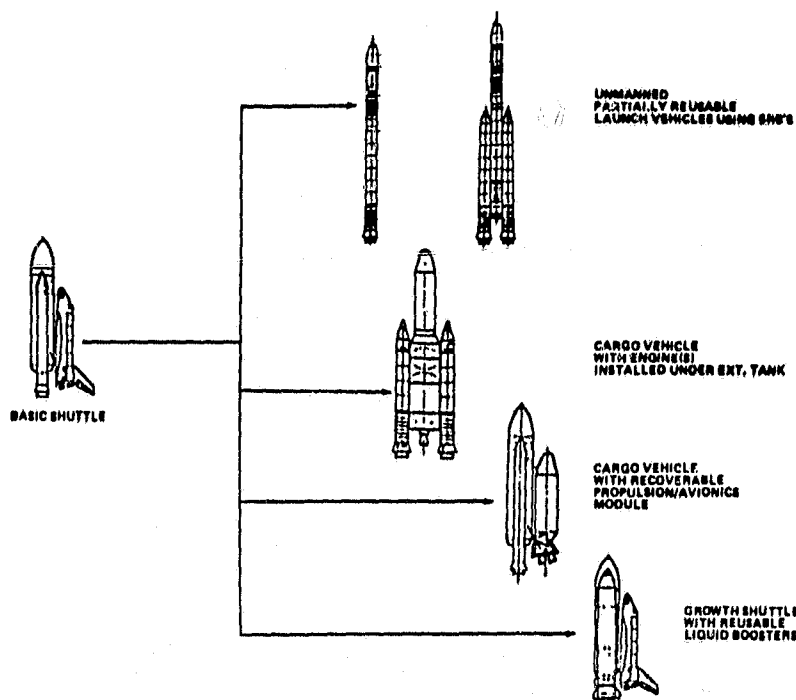


Figure 22. Shuttle-Derived Launch Vehicle Concepts Being Studied at MSFC

MSFC is currently investigating the use of flyback liquid rocket boosters on the Shuttle in order to reduce turn-around time and improve operational performance. Methane, propane, and RP were investigated as fuel for the Liquid Rocket Booster with propane and methane exhibiting a slight advantage. The replacement of the Orbiter with a cargo carrier and a recoverable, reusable Propulsion/Avionics module continues to be investigated as a launch vehicle with increased payload performance and increased payload volume capability. This Shuttle Derived Vehicle could supplement the STS Program.

ORIGINAL PAGE  
BLACK AND WHITE PHOTOGRAPH

Other launch vehicle concepts that are being investigated include the removal of the Orbiter and the placement of a single or dual SSME under the External Tank with the payload container mounted on top of the External Tank ("in-line" configuration) and the combination of Solid Rocket Motors to form an all-solid motor launch vehicle (except for the terminal stage).

In addition to studies to define SDV configuration options, emphasis is being placed on identification of technologies applicable to Shuttle-derived vehicles, and the degree of benefits to be derived from such technology advances. Technology areas identified to date include: (1) LOX/hydrocarbon propulsion technology, for potential application in reusable liquid rocket booster stages; (2) Structures, materials, and thermal protection systems (TPS) technology for potential reduction in weight, turn-around time and costs; (3) Avionics and recovery systems technology for the recovery of guidance, navigation, control and propulsion systems of the cargo vehicles; (4) Manufacturing and quality assurance technology for reduction in manufacturing time, testing and costs; and (5) Operations technology for the reduction of vehicle turn-around requirements and launch procedures. (M. Page/PS06/453-3425)

ORBITAL TRANSFER VEHICLES

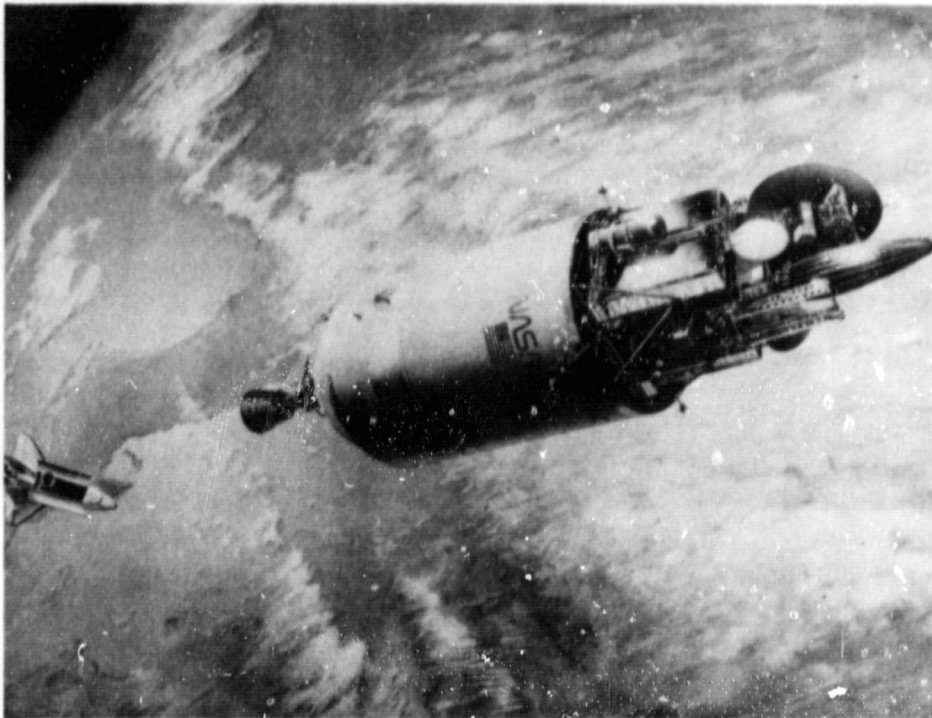


Figure 23. Orbital Transfer Vehicle



ORIGINAL PAGE  
BLACK AND WHITE PHOTOGRAPH

Studies conducted during this period identified the need for a very short stage which can deliver a very long and substantial mass to high Earth orbit. OTV concepts were identified and defined which use a toroidal oxidizer tank around the engine to minimize stage length. Studies are needed for the propellant management systems for this type of tank. An alternative concept has been studied which involves launching the OTV in an aft cargo cannister below the External Tank of the Shuttle, thereby freeing the total Orbiter cargo bay for payloads.

Technology studies aimed at improving the performance of cryogenic stages have been underway for several years and involve advanced engine studies, cryogenic propellant management breadboard testing, and cryogenic propellant tank design and verification. (D. Saxton/PS04/205-453-2796)

SOLAR ELECTRIC PROPULSION SYSTEM

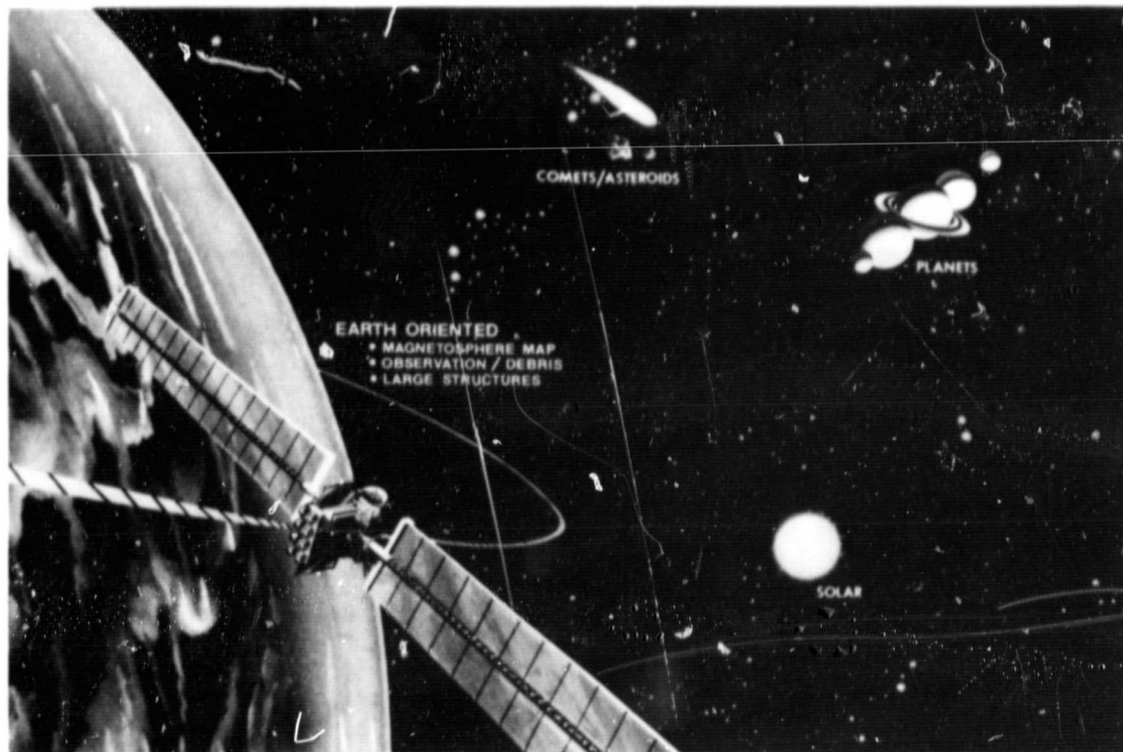


Figure 24. Solar Electric Propulsion Stage

This is an advanced system (Figure 24) for transferring payloads from low-Earth orbit into planetary and higher energy trajectories. In addition, it will provide power and other services to its associated experiment payloads. In support of the Phase B design activities completed in January 1981, MSFC has continued investigations in the key technology areas and

ORIGINAL PAGE  
BLACK AND WHITE PHOTOGRAPH

assumed responsibility from OAST/LeRC for the 30-cm Ion Thruster Technology Ready Program activities. Key technology areas investigated included: (1) enlargement of the experience data base for the current state-of-the-art transistors and capacitors to be used in the high power circuits of the 30-cm Ion Thruster Power Processor; (2) determination of solar cell performance for deep space missions including the performance characteristics of large area cells (This activity is covered in more detail in the Advanced Development Section.); (3) formulation of plans for future 30-cm Ion Thruster Particles and Fields testing based on the results of the LeRC tests in this area; (4) formulation of plans for a future solar array panel plasma power drain test; and, (5) application of low thrust mission/trajectory analysis for multiple asteroid rendezvous missions. In carrying out the activities of the 30-cm Ion Thruster Technology Ready Program, in-house repair of the power processors utilized to support the program have been accomplished as well as a broad range of thruster material and thermal investigations.

The Solar System Exploration Committee has recommended that the SEPS development proceed on a schedule that would support a 1990 launch of a Comet Rendezvous mission. This schedule would require SEPS development initiation in 1985. (J. Harlow/PF13/205-453-3322)

TELEOPERATOR MANEUVERING SYSTEM/REMOTE SATELLITE SERVICER

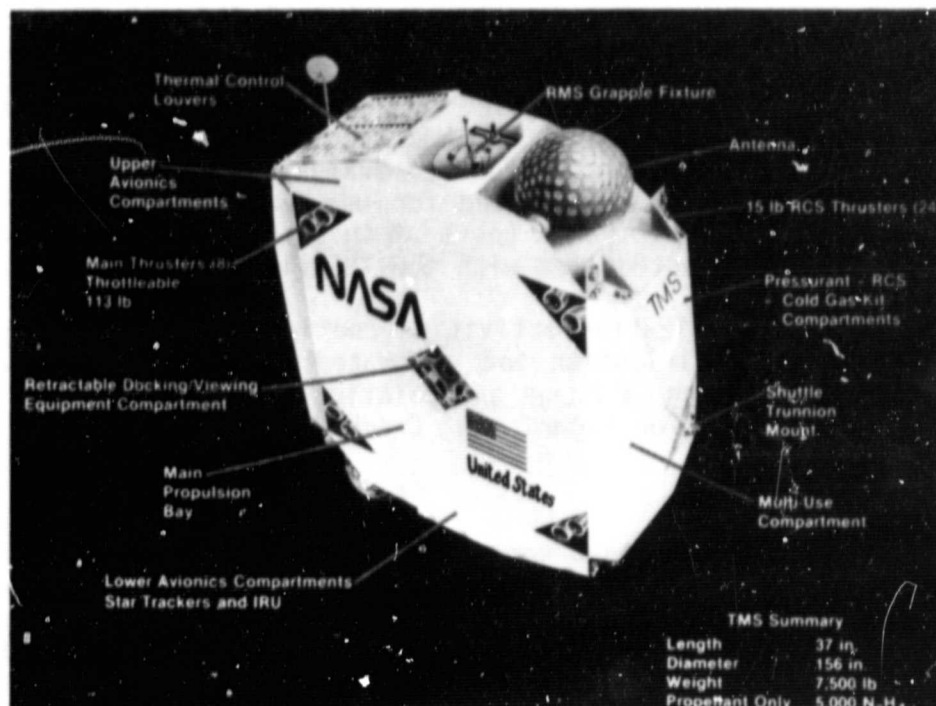


Figure 25. Teleoperator Maneuvering System

The Teleoperator Maneuvering System (TMS) Mission Requirements and System Definition Study which was initiated in June 1980 has been extended through February 1982. The TMS concept emerging to date is pictured in Figure 26. This system is capable of delivering and retrieving payloads and is compatible with the addition of certain mission kits to accommodate spacecraft remote modular servicing, structural assembly support and more autonomous robotic functions such as space debris retrieval.

The system is 37" long with a diameter of 156". Main propulsion is provided by eight 113-pound thrusters utilizing monopropellant hydrazine. The vehicle carries a total of 5,000 pounds of propellant (including RCS) and may be employed in a dual version which adds another set of tanks for a total propellant capacity of approximately 10,000 pounds. The basic system dry weight, including the docking kit, is 2,800 pounds. The TMS can place a 20,000 pound payload 500 n.mi. or a 5,000 pound payload 950 n.mi. above the Shuttle 160 n.mi. parking orbit. It is also capable of furnishing round-trip support to payloads - typically it can deliver and return a 10,000 pound payload 440 n.mi. above the 160 n.mi. orbit. Man-in-the-loop remote control is provided from the Orbiter aft flight deck or from the ground via TDRSS.

The concept is designed to enhance the STS services/capabilities by providing propulsive performance, more flexibility for multiple payload manifesting, and satellite services/operations support in orbits beyond the Shuttle's capability or where dynamic disturbance/payload contamination requirements constrain "close-in" Shuttle operations. Supporting development activities during the year include purchase of an RMS end-effector and grapple fixture from SPAR which is being evaluated for use as a docking mechanism using the air-bearing floor facility and also the six-degree-of-freedom motion system simulation facility at MSFC. The air-bearing floor five-degree-of-freedom facility was used to continue evaluation of the MMS berthing interface for docking and this MMS simulation is being adapted to the six-degree-of-freedom system for further evaluation.

The short range CW radar was adapted for use as a terminal rendezvous/docking radar sensor for TMS. Bench tests of this system have been successful and the unit is being integrated with the TMS simulator for active docking simulation tests.

Television system utilization activities continued through the year in the areas of target identification and automated terminal docking control systems techniques utilizing TV range and pointing data which has the potential of obviating the need for radar. (D. Cramblit/PS04/205-453-0367)

#### Command And Telemetry Link

MSFC has developed an upgraded command and telemetry data system for the Electronics and Control Laboratory Teleoperator Maneuvering System Simulator. The system serves as a combination transmitter and receiver for discrete command data and analog measurement data. The transmitter half converts 64 discrete inputs and 6 analog inputs to a formatted serial baseband signal suitable for modulating a telemetry transmitter. The receiver half accepts a demodulated signal from another command and telemetry unit and reproduces the 64 discrete signals and 6 digitized analog signals. The receiver and transmitter operate independently; however, both are driven by

a single microcomputer capable of managing both tasks concurrently at the given 2000 bits per second data rate. Two such units have been built: one is a battery-operated unit for the mobile teleoperator unit itself; the other is an AC unit for the command console. (D. Harris/EC33/205-453-1570)

#### Signal Processor for FM-CW Radar

MSFC has developed a microprocessor based signal processor which provides range and range-rate readouts for remote vehicle docking purposes. This processor in conjunction with a 35 GHz FM radar is capable of deriving accurate close-in range measurements in the 0.5 meter to 20 meter range. The technique utilized significantly reduces the "step" error normally encountered with FM-CW radars with a given sweep width. Averaging from 1 to 16 range counts serves to smooth the digital range readout. Range-rate is mathematically derived from successive range counts by the microprocessor. (E. Gleason/EC33/205-453-1570)

#### GRAVITY PROBE B

Gravity Probe B, containing the Relativity Gyroscope Experiment, is one of the few known laboratory tests of general relativity. The experiment seeks to measure two components of the precession of a gyroscope as predicted by the general relativity theory. The precession is small. In the low Earth orbit proposed for Gravity Probe B, the largest component, the geodetic effect, is 6.9 arc sec/year while the smaller, the motional or gravimagnetic effect, is only 0.050 arc sec/year. The gravimagnetic effect is the gravitational analog of magnetism. Neither its magnitude nor even its existence has ever been demonstrated in any other test of relativity. Only in a satellite where the support forces on the gyroscope can be minimized is it possible for the relativistic precession to dominate that from classical sources. The measurement of the geodetic effect to the proposed accuracy of 0.001 arc sec/year is a factor of 30 more accurate than any previous test. Such accuracy will permit the testing of relativity theories with unprecedented precision. Observation of the gravimagnetic effect should provide clues to the nature of quasars, the most powerful sources of energy in the Universe. The Space Science Board's report on Gravitational Physics identified the detection and accurate measurement of the gravimagnetic effect as the number one priority for space relativity in the 1980's.

In the fall of 1980, MSFC initiated an in-house systems definition of the GP-B spacecraft. This activity is supported by Stanford University which is the parent organization of the Principal Investigators for this experiment. The impetus for starting this effort was provided by the recommendations of the Rosendhal Committee (a peer review committee that assessed the technology readiness of this project) which stated: "The Program is now ready to proceed into a new phase which will emphasize system studies and engineering development on a well-defined schedule leading to design of the final flight experiment." Since the initiation of this study, MSFC and Stanford have completed a number of system/subsystem trades, and a

ORIGINAL PAGE  
BLACK AND WHITE PHOTOGRAPH

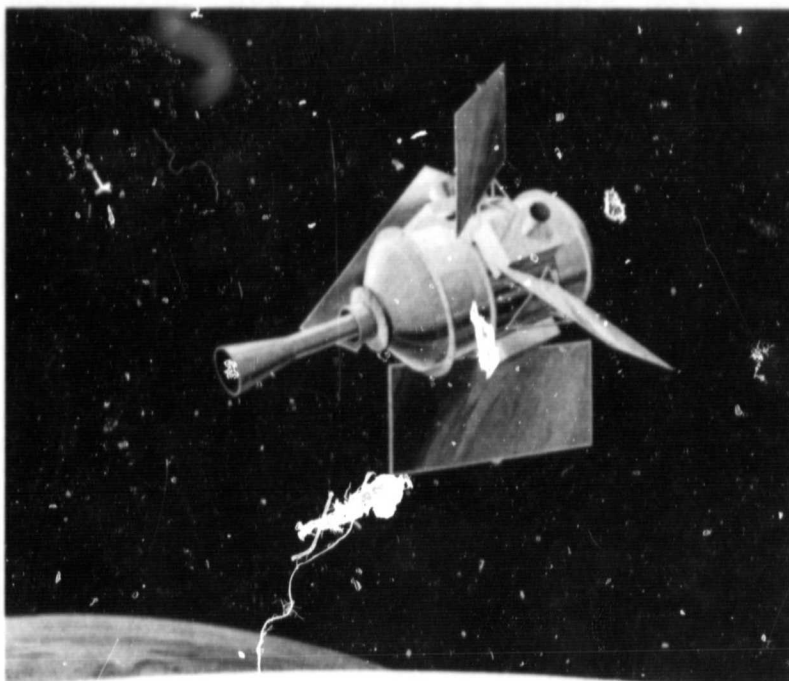


Figure 26. Gravity Probe B

configuration on which preliminary design can begin will be selected in December. Current programmatic and technical planning is being formulated against an assumed FY 1984 new start.

The definition study is supported by an extensive parallel advanced development effort at Stanford and MSFC. During the past year, emphasis at MSFC has been on: the development of techniques to polish a very homogeneous quartz ball (the rotors for the experiment gyroscopes) to extremely accurate sphericity (approximately 1 millionth of an inch) and the development of measuring techniques to verify the sphericity; the design and development of a technique and the equipment to accurately coat the quartz rotors with a uniform thin (approximately  $2500 \text{ \AA} \pm 75 \text{ \AA}$ ) layer of niobium; and a program to understand and characterize the bonds resulting from optically contacting quartz pieces, which is the proposed method for assembling the instrument that contains the experiment gyroscopes. (A. Neighbors/PF16/205-453-1232)

#### ADVANCED X-RAY ASTROPHYSICS FACILITY

Pre-phase B activities continued during FY81. These activities included several systems analyses supporting the reference concept for AXAF, supporting technology, including continued operation of the X-ray Test and Calibration Facility to measure the X-ray scattering properties of selected flat

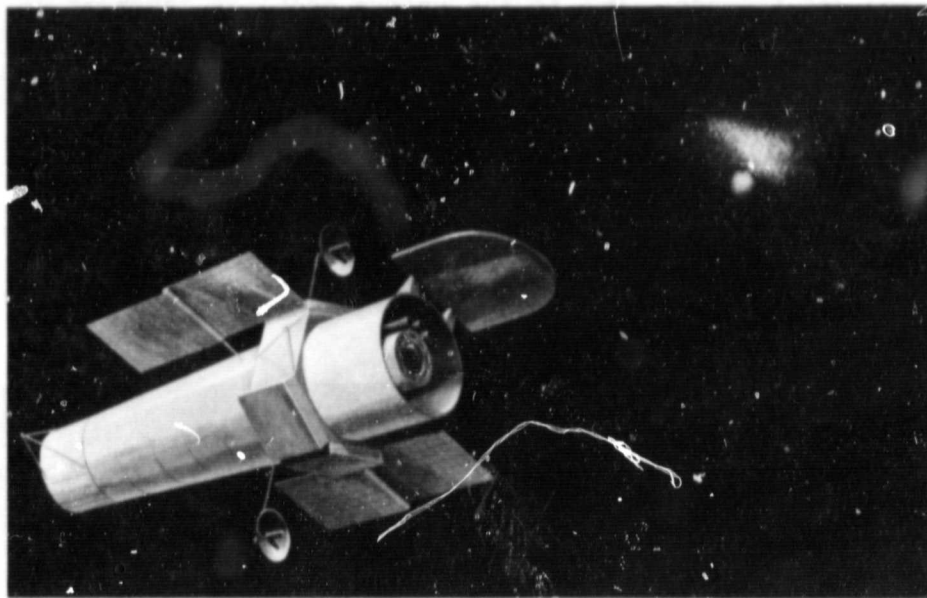


Figure 27. Advanced X-Ray Astrophysics Facility

samples of candidate materials for the AXAF mirrors, and detailed program planning. Two specific examples of progress in technology are the completion of preliminary versions of an X-ray scatterometer and heterodyne profilometer. The scatterometer measures local scattering at X-ray wavelengths on reflecting surfaces. The profilometer uses a visible light laser in a configuration which permits rapid data gathering and display of the surface characteristics of the sample. Both instruments are presently limited to flat surfaces, but will be modified during the next year to permit measurements on curved surfaces such as the cylindrical optics of AXAF. These techniques show considerable promise in making it possible to obtain the surface figure and smoothness properties required to meet AXAF mirror performance goals. (C. Dailey/PS01/205-453-0162)

#### PINHOLE OCCULTER FACILITY

This system is intended to be a Space Shuttle-based facility to produce the hard X-ray images generated by the Sun. It is basically a pinhole camera using a 50 meter deployable boom to separate the pinhole device from instrumentation in the Shuttle (Figure 28). At the far end of the boom will be a fifty kilogram mask containing two sets of pinhole arrays and two chronograph shields. At the near end of the boom, the instrumentation and a gimbal pointing system are located. An ad hoc science working group composed of solar astronomers has developed the science objectives and defined performance requirements to satisfy them. Pointing and control studies have



demonstrated the feasibility of attaining the desired pointing accuracy of less than ten arc-seconds. Due to the unique problems inherent in controlling a long, relatively flexible body to these accuracies, it is necessary to utilize modern control techniques. Evaluation efforts have demonstrated such a scheme which controls predominant bending modes and suppresses less sensitive modes to obtain the desired pointing stability. Sophisticated digital controllers are required in the pointing and control system. Other studies have identified configurations for providing acceptable levels of diffracted and scattered background light ( $< 5 \times 10^{-11}$  solar brightness). Preliminary systems requirements have been identified and implementation of all requirements seem very feasible. (J. Dabbs/PS02/205-3430)

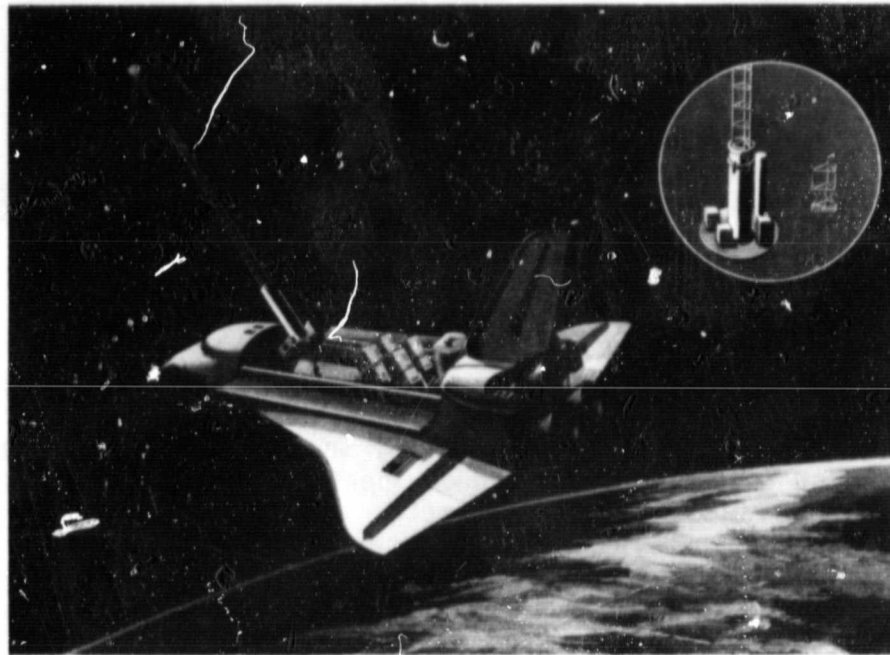


Figure 28. Pinhole Occulter Facility

#### TETHERED SATELLITE SYSTEM

Following concept initiation by the Smithsonian Astrophysical Observatory in 1974, early conceptual definition studies were accomplished by MSFC, including formulation of the basic control law for closed loop control of the system. System definition studies were carried out from 1977 to 1980. User requirements studies were also carried out by a Facility Requirements Definition Team comprised of scientists from various government and university communities. The Office of Space Transportation Systems, the Office of Space Science, and the Office of Space Terrestrial Applications have supported these studies. Plans are now being formulated for development of the

system to be used for the initial demonstration/verification flights and, subsequently, as a science facility for flights in the late-80's and beyond. (J.Laue/PS01/205-453-4570).

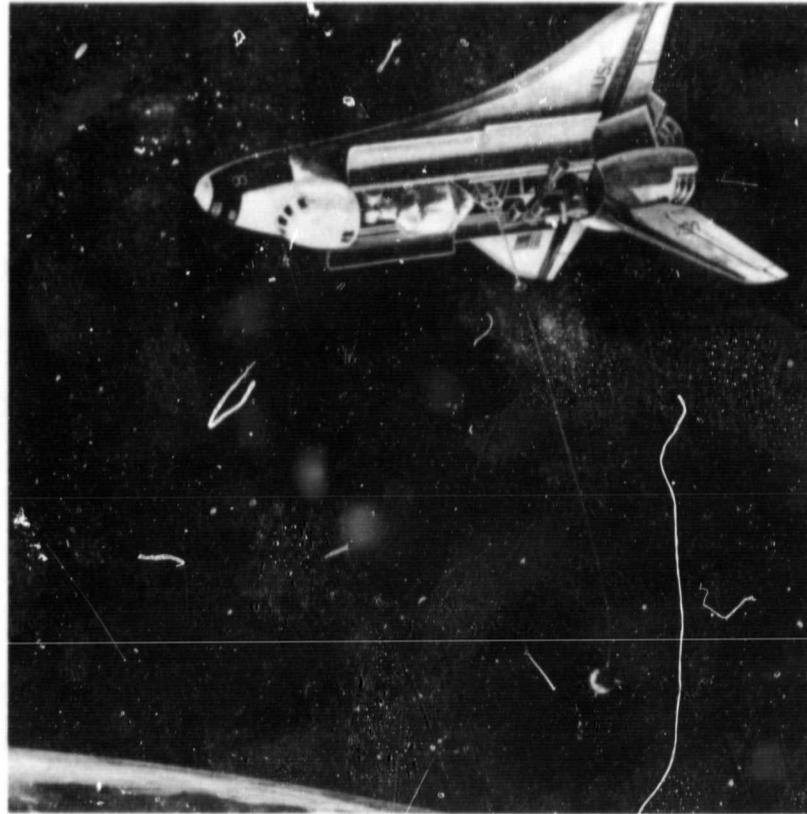


Figure 29. Tethered Satellite System

#### LARGE SPACE SYSTEMS

The purpose of the large space systems research is to develop and demonstrate the technology needed to build large structural systems in space. Two principal construction categories exist for achieving this purpose. They are the space fabrication and the deployable methods. The Composite Beam Cap Fabricator is an example of a space fabrication activity and the SASP Deployable Truss (Figure 32) is an example of a deployable activity. To support the space fabrication and deployable work several testing activities are underway. The ground testing to determine the dynamic behavior of a 1-meter aluminum beam that has been manufactured in the automated beam builder is an example. Prospective space systems that may use this technology are the Deployable Antenna, Second Order Science and Applications Space Platform and the Experimental Geostationary Platform.



Space Platform

The Space Platform (SP) is a free-flying, unmanned platform (see Figure 30) in low Earth orbit that supports science and applications payloads attached to it by providing electrical power, heat rejection, communications and attitude control. Periodically, the Space Shuttle will berth to the SP for payload module replacement, exchange and/or maintenance and repair. This Shuttle support mode will also be used for SP maintenance and repair. The SP can provide resources to the Orbiter for extended durations if required for these operations. These same resources could also be used to extend the duration of Spacelab sortie missions.

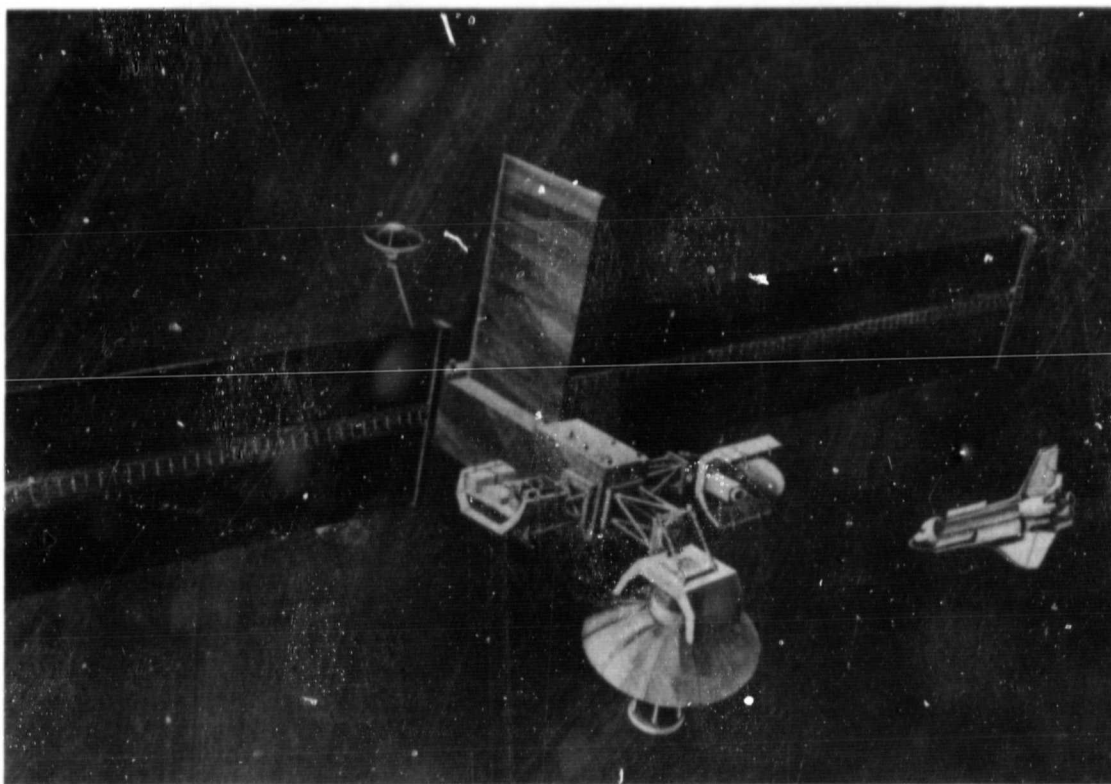


Figure 30. Space Platform

The SP has inherent growth capability which can be evolved through several program paths. Because of the modular design, the initial SP can be replicated in different sizes and placed in different orbits to meet specific user needs. Enhanced unmanned platform capability can be obtained through the orbital attachment of deployable structural arms that would provide additional berthing ports and increased payload spacing. The SP also provides the initial core element of a manned station. The evolution is discussed later in this report.

Definition studies (Phase B) of the Space Platform were completed in August 1981 by MDAC and TRW. Also, in parallel to these studies were supporting studies on the solar array by LMSC and TRW. These studies produced the configuration and program planning definition required to initiate development phase in FY 1983. This would lead to a projected availability in mid-1987. In the interim period, the contractors are continuing studies in critical areas and building mockups and test articles of key items to minimize the development risk and cost.

During 1981, in parallel with the contractors, MSFC continued advanced development activities in several areas. Of particular significance are the development of a Programmable Power Processor (P<sup>3</sup>) for use as a battery charger and regulator, testing of a power system breadboard, and the initiation of life-cycle testing on CMG bearings and slip rings. In support of the growth space platform, MSFC is pursuing advanced development efforts in large deployable space structures including fabrication and testing of ground test articles. These activities are reported in more detail in the next sections. (L. Powell/PM01/205-453-5310)

### User Requirements

During the past year, significant changes in direction have been made in defining the Space Platform. The 25 kW Power Module (PM) and the Science and Applications Space Platform (SASP) have now been combined into a single system called the Space Platform. This initial 12 kW Space Platform is a relatively simple platform capable of supporting meaningful scientific investigations. After carefully reviewing the science and applications requirement and the availability of instruments and facilities in the 1987 timeframe, our current approach is to define requirements for this initial Space Platform as a first step in an evolutionary program. This initial Space Platform would provide: accommodation for high priority science; a demonstration of on-orbit servicing and payload exchange for the space platform; conduct of multidiscipline investigations; and the evolutionary potential for future space platforms. That is, the initial Space Platform should demonstrate the essential features of the platform concept and allow evolution to take place through expansions of concepts demonstrated on the first platform and implemented on new flight hardware systems or refurbishment of hardware in the initial Space Platform system. The results of these activities will be presented to the NASA Council during the review of FY83 new starts. (C. DeSanctis/PS02/205-453-3430)

### Manned Space Platform

The availability of the Space Platform (SP) in the mid-1980's in combination with the Shuttle/Spacelab systems and subsystems, will enable a transition from the Spacelab sortie mode of manned operations to a permanent manned presence in low Earth orbit (Figure 31). Studies were initiated this past year to define approaches and concepts for a manned space platform. The concept would use the Space Platform as the basic resource module; a habitability/experiment module which could be derived from Spacelab; and crew equipment developed for the Shuttle and existing systems. The Space Platform will be operational in the 1987 time-frame supporting unmanned

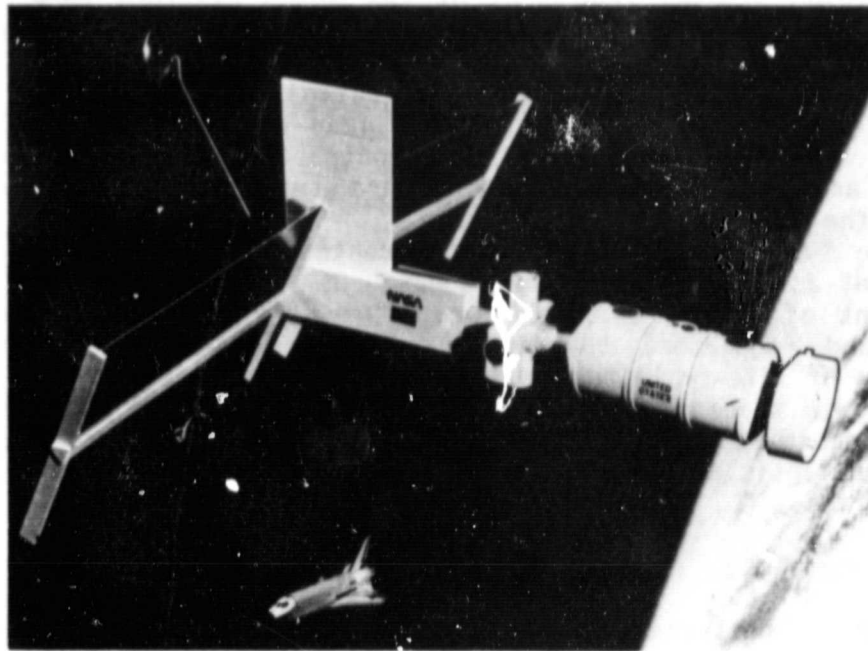


Figure 31. Manned Space Platform

science and applications missions. The manned space platform, which could be available in the late 1980's, would be assembled from elements carried to orbit by the Space Shuttle and would utilize a replication of the initial Space Platform. The manned space platform will provide a permanent presence in space which will be utilized for science and applications missions, such as solar terrestrial observations, life sciences and materials processing, and will provide a test-bed for future space operations, such as large structures deployment/assembly/construction, spacecraft servicing and propellant refueling of orbit transfer vehicles. (C. Priest/PS04/205-453-2769)

#### Deployable Platform Activities

A Deployable Truss, designed to meet the requirements of an early version of SASP, has been fabricated and delivered to MSFC. This truss is designed to be automatically deployed, requiring no assistance from the remote manipulator or an astronaut. Electrical power, data and communication cables, fiber optics, and the Deployment Drive System will be installed for functional, structural, and vibration testing at MSFC.

A representative deployable structure, measuring 3m x 3m x 15m when fully deployed, has been fabricated and tested in the Neutral Buoyancy Simulator at MSFC. Deployment was achieved by use of a simulated remote manipulator assisted by suited Test Subjects. These tests have provided verification of the design and timelines for orbital operations involved in the deployment. (E. Engler/EP13/205-453-3958)

ORIGINAL PAGE  
BLACK AND WHITE PHOTOGRAPH

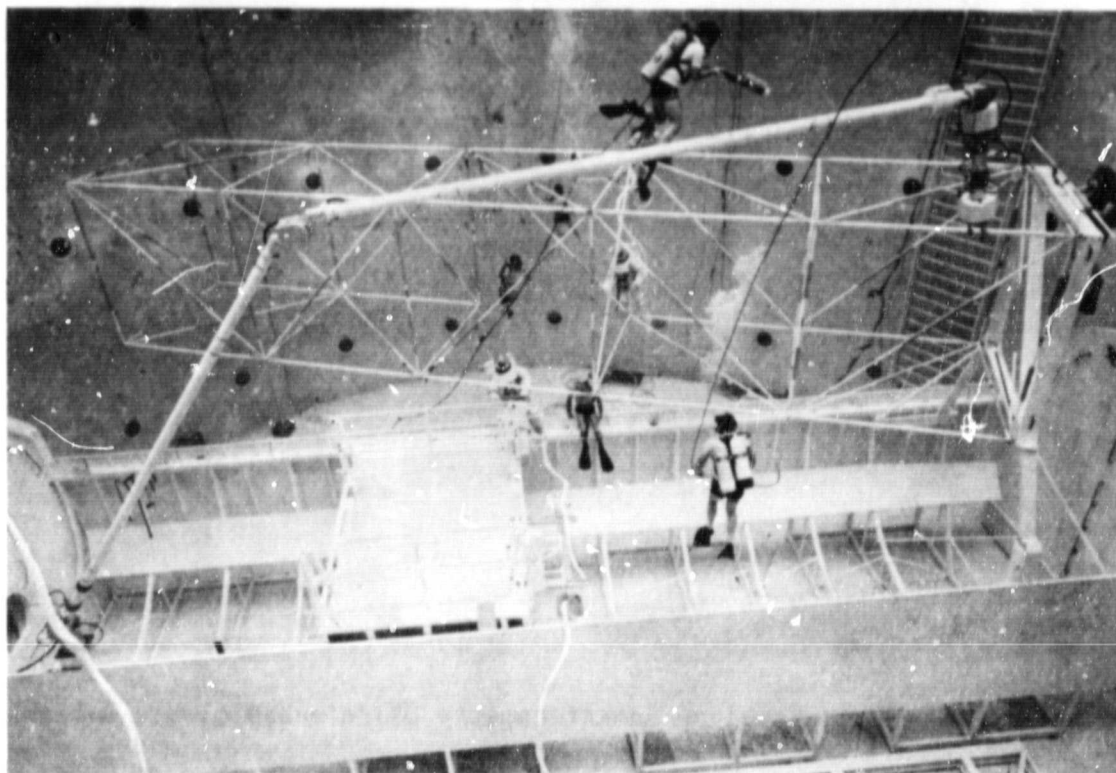


Figure 32. Expandable Large Space Structures

Deployable Antenna Flight Experiment

System Definition Studies during FY81 produced preliminary designs and program plans for a large aperture engineering flight test and measurement program in low Earth orbit on the Shuttle Orbiter. The 50-meter antenna test program is configured to provide technology support for future space applications which utilize large structures deployed directly from the Shuttle or upper stages. The flight system is configured as a reusable test-bed facility to evaluate structural and electronic characteristics applicable to advanced civil and military system designs with 50-200 meter apertures. Primary verification tests are zero-g deployment and measurement of dimensional accuracy and stability of the antenna structure under varying thermal environments and attitude control excitations. Additional design definition on control dynamics of the Orbiter-attached antenna is providing further data on large structures control by the Orbiter. The evaluations on radio frequency and structural measurements are directly applicable to technology needs for multi-users in areas of communications, radar, radiometry and radio astronomy. (W. Thompson/PS04/205-453-2796)

ORIGINAL PAGE  
BLACK AND WHITE PHOTOGRAPH

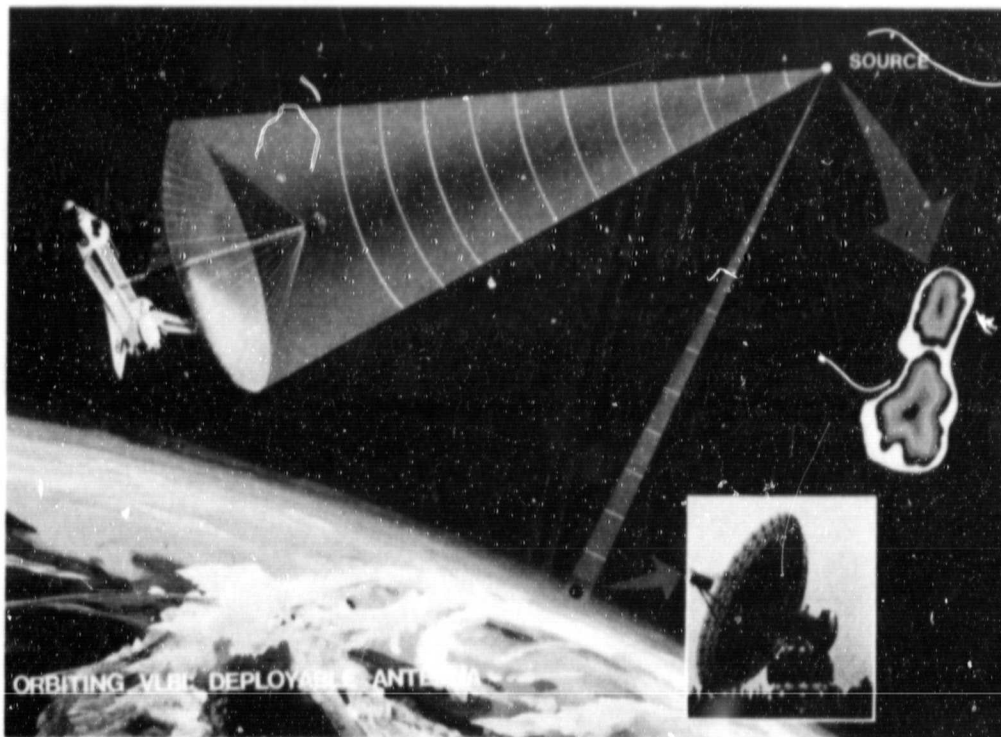


Figure 33. Very Long Baseline Interferometry Using a Deployable Antenna

Very Long Baseline Interferometry Experiment

Dramatic improvements in the angular resolution of the brightness distribution of extra-galactic radio sources have been achieved in recent years by using interferometric techniques. These techniques use widely separated radio telescopes. An Orbiter based flight experiment using a large deployable antenna would provide an opportunity to extend interferometry into space. This antenna would be one of the observing antennas in conjunction with one or more on Earth. Received signals would be heterodyned to a video frequency and recorded at each receiving antenna. As the Orbiter circles the Earth, individual recordings for each individual object of interest would be made. By correlative analysis of these recordings, spatial Fourier components of the brightness distribution of celestial objects can be obtained. These can be used in turn to construct high resolution maps of the objects, from which can be inferred valuable data about the physical processes occurring in quasars, active galactic nuclei, galactic masers, and other objects of interest.

During 1981, a technical working group was established to assist in the science and mission design of a Very Long Baseline Interferometry (VLBI) experiment. Scientific objectives and mission and system/subsystem requirements for performing a VLBI demonstration have been established. (S.Morgan/PS02/205-453-3430).



### Experimental Geostationary Platform

Studies to determine the feasibility of concepts for Operational Geostationary Platforms for the 1990's were completed. The benefits of using platforms in lieu of single purpose satellites were also studied resulting in the conclusion that platforms offer economic benefits, and platforms offer a potential solution to the orbital arc and frequency spectrum problem currently being experienced. These platforms would accommodate a variety of U.S. Domestic and International missions providing for projected traffic in such service areas as long distance telephone, data/facsimile transmission and video links. Advanced meteorological missions as well as DOD missions could also be accommodated on these platforms.

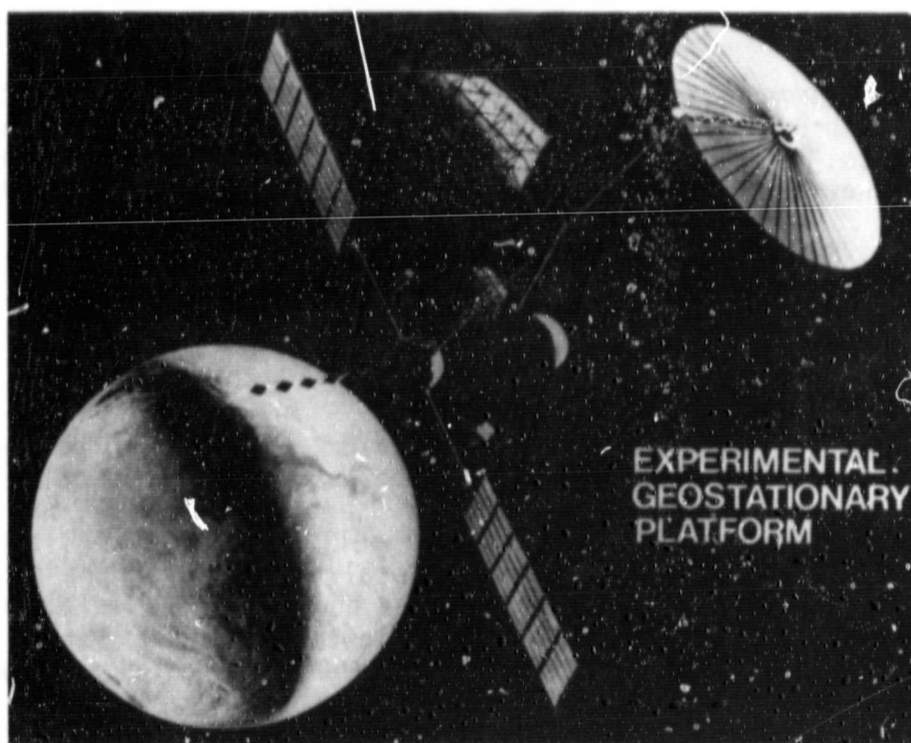


Figure 34. Experimental Geostationary Platform

NASA's interest in these platforms is to develop and demonstrate during the 1980's the technologies and systems capabilities necessary for operational platforms of the 1990's. More efficient power generation, storage, distribution, and central systems are needed. Advanced long life components (such as batteries and momentum wheels) and low coefficient of thermal expansion structures are required. Large structures require distributed active attitude control systems. The transfer of large spacecraft from LEO to GEO together with remote rendezvous, docking, and hot servicing must be

demonstrated. New communications technologies requiring demonstration include multibeam antennas with reconfigurable beam forming networks to provide frequency re-use; on-board processing and switching; interplatform links; pointing accuracy for narrow beams; propagation characteristics of multi-beam antennas at C, Ku, and Ka Band, etc.

Concepts which would demonstrate these technologies and systems capabilities were studied (Figure 34). A NASA Briefing and Workshop on Geostationary Platforms was held in March 1981. This workshop, attended by virtually all major U.S. commercial and Governmental organizations currently involved in space communications, identified and defined institutional, technical and operational issues associated with operational geostationary platforms. Studies of the Experimental Geostationary Platform have been supported by both the OSTS and OSTA. (W. Carey/ PS06/205-453-3424)

## SPACE TECHNOLOGY

The accomplishments of the Center in its technology projects reflect the major roles in propulsion systems, materials and processes, electrical power and electronics. Steady progress is being made in each of these areas, with thorough engineering practices being followed and applied throughout.

## CHEMICAL PROPULSION SYSTEMS

### Shuttle External Tank

Some method was required for the Shuttle External Tank to determine whether the insulation was properly bonded to the metal substrate. The technique that was developed involves the use of a device to apply a very low force pulse that is measured by a load cell. The load cell signal is a direct and instantaneous measure of the local stiffness of the material at that point. If the insulation is not well bonded to the metal substrate, the stiffness of impedance will be much lower causing a longer duration pulse or vice versa. Spectrum analysis of the pulse obtained from a well bonded point will display frequencies 425 Hz and above. Spectrum analysis of a pulse obtained from a partially debonded point will only show frequencies below 425 Hz because the insulation alone (not well bonded) does not have the stiffness to support energy at the higher frequencies.

The equipment used consists of an HP 5423A Structural Dynamic Analyzer, HP 9826A Desktop Computer and a custom impact device with a PCB load cell/amplifier. The Fast Fourier Transform Analyzer is perhaps the most important piece of equipment in the system. It takes the time histories and makes the frequency conversion in approximately two seconds. The Desktop Computer determines the termination frequency of the force auto power spectrum and displays the grade of the bond in a matrix. The system calibration, bond grade, matrix size, and measurement point sequence are all predetermined by interactive setup questions in the Desktop Computer. (G. Johnston/ET19/205-453-1320)

## Automation of Solid Rocket Design

An improved pattern-search technique was utilized in a computer program which minimizes the sum of the squares of the differences, at various times, between a desired thrust-time trace and that calculated with a mathematical performance model of a solid-propellant rocket motor (SRM). Up to 14 design parameters may be varied during the search. These parameters fix the design of the SRM which may consist of various common grain configurations. The large number of designs that must be evaluated during the search for the "best match" of calculated to desired performance necessitates the use of a relatively simple model of the SRM's performance. The model selected provides the required data for a single design on the IBM 3031 computer in about 10 seconds of operating time. Important features of the model are an approximate evaluation of the effects of grain deformation on burning surface geometry and an empirical equation which determines propellant burn rate in terms of the zero crossflow-velocity burn rate and SRM operating pressures, geometry and flow parameters. The performance model has shown good quality predictions for five existing SRM's of very different sizes and configurations. The overall program was demonstrated by matching the thrust-time trace obtained from the static test of the first Space Shuttle SRM starting with input values of 10 variables which were, in general, 10% different from the as-built SRM. An excellent match was obtained; final design parameters were for the most part within a few percent of the as-built values.

Sforzini, R. H.: Automated Approach to Design of Solid Rockets. J. of Spacecraft and Rockets, May - June 1981, 200.

## Shuttle Solid Rocket Motor Nozzle Ablative Evaluation

Recent nozzle design and test activities have identified six new nozzle ablatives with outstanding performance. These ablatives utilize spun PAN and continuous pitch and PAN fibers in lieu of the continuous rayon fibers used in the Shuttle Solid Rocket Motor (SRM). Approximately 13,600 lb. of carbon cloth phenolic prepreg material is required to fabricate each SRM nozzle. If recession rate and char rate performance can be improved or if material costs can be reduced, a proportional benefit to the Shuttle Program can be achieved due to the enormous quantities of ablative required. Candidate ablatives discussed in this paper have demonstrated superior performance throughout subscale testing. Projected costs are 40% lower in the mid-80's.

Availability of baseline continuous filament rayon precursor has been a concern during the Shuttle program due to the relatively small volume of rayon required by the aerospace industry. The concern is that the volume requirement may be insufficient to ensure continued profitability and retention of the supply source. Pitch is an attractive precursor for carbon and graphite fibers because it is readily available, low in cost, has a high carbon content, and requires a relatively minimal amount of energy for conversion into a pyrolyzed product. Likewise, PAN is attractive because it has a stable market, is low in cost, has a high carbon content and has multiple producers.



The objective is to build up the data base on these potential SRM nozzle ablatives to support an ablative selection and the design of a 10-inch throat diameter test nozzle. The 10-inch nozzle test effort will precede and support a full scale SRM improved nozzle qualification. Sensitivity to propellant solids loading is evaluated by comparing nozzle performance using three propellants, viz 86% solids - 16% aluminum PBAN, 86% solids - 18% aluminum HTPB, and 88% solids - 18% aluminum. A complete characterization of the selected ablatives will be performed as a part of the 10-inch throat diameter fabrication and test.

Subscale tests suggest a lower cost ablative can be substituted for the rayon based carbon ablative now used in the Shuttle SRM nozzle. Graphitized pitch performed best in the tests accomplished to date. Based on this, a reduction in recession of approximately 40% over the present baseline ablative could be expected. Continuous and spun PAN likewise out-performed the baseline ablative by approximately 15%. Six tests to demonstrate the Shuttle low cost nozzle concept using a lightweight insulator spacer ring were successful. Structural integrity of the lightweight insulator was satisfactory even though the insulator was severely charred in some cases.

1985 prices for pitch and PAN ablatives are projected to be \$20.00 to \$30.00 per pound based on the establishment of an expanded market for these materials. Whereas the presently used rayon precursor carbon ablator market projections indicate a rising cost trend. A 1985 price of \$40.00 to \$45.00 per pound is estimated primarily due to the relatively small volume requirement for rayon. Incorporation of low cost nozzle ablatives potentially could reduce present raw material cost by \$548,000 per Shuttle launch. Additionally, reduction in liner recession can significantly improve the nozzle performance. A specific impulse gain of 0.6 sec. is predicted based on the reduced liner erosion which corresponds to a Shuttle payload gain of 500 lb. Another payload gain of 213 lb. is projected in conjunction with the 1173 lb. nozzle weight reduction for the low cost nozzle design. The improved nozzle efficiency and weight reduction together are predicted to provide a total Shuttle payload gain of 713 lb. (L. Powers/EP25/205-453-3809)

Powers, L. B., and Bailey, R. L.: Shuttle Solid Rocket Motor Nozzle Alternate Ablative Evaluation. AIAA/SAE/ASME 17th Joint Propulsion Conference, Colorado Springs, CO, July 27 - 29, 1981.

#### Concentric-Chamber, Dual-Throat Thrust Chamber

Investigations continued of an engine having a thrust chamber employing concentric combustors and nozzles which can change area ratio and thrust during its operation without employing large translating nozzle extensions. This capability can provide an improved method for tailoring propulsion system performance to vehicle mission needs. The thrust chamber operates in the launch mode by having both combustion chambers operating. For altitude operation, only the inner, primary chamber operates reducing the effective throat area, thus increasing area ratio and performance.

ORIGINAL PAGE IS  
OF POOR QUALITY

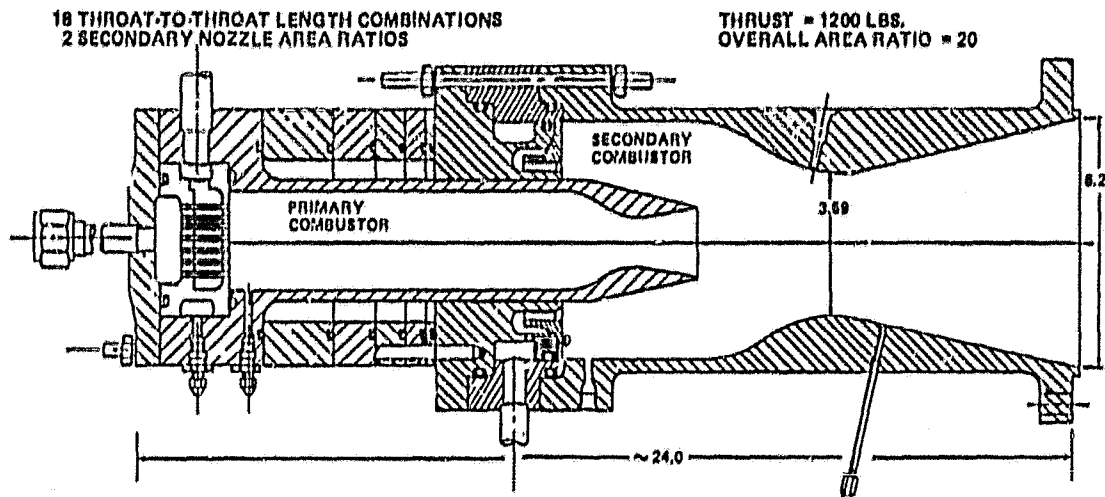


Figure 35. Uncooled Dual Throat Test Rocket Engine

The first hot tests of this thrust chamber concept have been successfully conducted in-house at low mixture ratio and have verified aerodynamic data from previous cold flow tests. The previously constructed internal aerodynamic model for this type chamber has been modified to improve its analytical techniques and data handling capability. Preliminary chamber cooling requirements for a baseline dual-throat engine system have been determined analytically leading to the start of construction of a dual-throated thermal model (Figure 35). (F. Braam/EP24/205-453-4827)

#### MATERIALS AND PROCESSES

##### Combined Specular/Diffuse Surface Thermal Technology Advancement

A comparison was made of methods used to analyze reflected energy when considering the specular (mirrorlike) as well as the diffuse component of a material's thermal-optical properties. Of particular concern was the specular reflection of solar energy from a non-planar surface and its distribution on a nearby planar surface. Three methods that were compared were a generalized thermal radiation program (TRASYS II), a specialized specular ray trace program, and a generalized Monte Carlo-based thermal radiation program.

Comparison of the three methods was made with regard to both analytical utility and accuracy. A technique was devised to smooth the reflected, discontinuous heat distribution, which is characteristic of specular analyses of non-planar surfaces. Although further work is needed, a methodology is now available for the thermal assessment of payloads with combined specular and diffuse surfaces. (L. Turner/EP45/205-453-3629)

#### Acoustic Environmental Accuracy Requirements for Response Determination

Two popular and effective techniques for structural/acoustic interaction analysis are modal analysis and statistical energy analysis. In recent years, many researchers have used these techniques to obtain adequate answers to noise transmission problems similar in nature to that posed by the Space Shuttle Payload Bay. Unfortunately, the computer codes devised to implement the mathematical techniques have been single-purpose, research-oriented programs. Each new problem has required a new or heavily altered program for solution by these techniques. To overcome this limitation, the most versatile modal analysis and statistical energy analysis formulations were identified and modified to form the basis of a general purpose, user-friendly computer program. The program makes use of the most advanced computer techniques available, including dynamic storage allocation, automatic core sizing, free-field alphanumeric reads, and the incorporation of a data complex. (S. Guest/ED24/205-453-1841)

#### Second Generation Sprayable Ablator for Solid Rocket Booster

A second generation sprayable ablator system, designated MSA-2, developed and tested in the Materials and Processes Laboratory is a versatile replacement for the current Solid Rocket Booster ablator, MSA-1, now being routinely applied to flight hardware in the KSC spray facilities. There are four desirable characteristics of this new ablator. First, it is applicable in greater thickness than its predecessor, the MSA-1. The MSA-2 solvent/resin/filler formulation contains a small quantity of ground cork that affords stress relief from elevated temperature cure to stresses. These same stresses consistently produced crack formation during cure of MSA-1 in thicknesses greater than 1/4". MSA-2 may be applied up to 1/2" thick, and will replace extensive areas of handbonded cork insulation. Second, it can withstand higher aeroshear/thermal stresses than MSA-1. The cork filler contributes to improved thermal resistance, and two of the three candidate resin binder systems are epoxy resins with inherently higher thermal stability. Third, it has a potential for cryogenic applications. The cork filler stress relief phenomenon contributes to structural integrity under cryogenic load. Fourth, it is designed to be compatible with the same spray application system used for MSA-1. No basic equipment changes will be required at KSC to adapt to the improved ablator. (W. Hill/EH43/205-0643)

## Multi-Layer Insulation System

A multi-layered insulation system has been designed for the Space Telescope that has three significant design goals. First, it meets specified performance values at minimum weight. Second, it is both cheaper and more quickly manufactured. Third, the design provides for more consistency of manufacturing and installation. The basic design uses an integrated sub-blanket. Each blanket assembly is made from three "subblankets" allowing for overlapping and off-setting of seams and fasteners. This minimizes the major sources of performance degradation.

Mating fasteners for the blankets are attached at the time of installation, thereby eliminating the need for tight dimensional control over the blanket. Both weight and time are minimized through the use of an ultrasonic welder to cut and seal the blankets. The welder permits complex shapes to be fitted in a single operation.

Recent tests have verified that this design provides a multi-layered insulating blanket that performs very close to the theoretical design limit. A blanket of twelve layers will meet the Space Telescope design requirement of effectance emittance  $< 0.01$ , after allowing for some handling and installation degradation. (A. Clayton/TA01/205-453-0480)

## Evaluation of Corrosion Protective Systems on Aluminum

A study of several protective coating systems for use on aluminum in seawater/seacoast environments has been conducted. This study was conducted to review the developments that have been made on protective coatings since early in the Space Shuttle program and to perform comparative studies on these coatings to determine their effectiveness for providing corrosion protection during exposure to seawater/seacoast environments. Panels of 2219-T87 aluminum were coated with 21 different systems and exposed to a 5% salt spray for 4000 hr. Application properties, adhesion measurements, heat resistance and corrosion protection were evaluated.

Examination of the results of these tests shows that outstanding protection can be afforded to 2219-T87 aluminum alloy in severe seacoast/seawater environments. Although the extensive evaluation of the presently used coating system utilized on the SRB has indicated very good protection for these environments, these tests indicate that some greater degree of protection would be expected by several of the coating systems evaluated. From this study, it also appears that chromates are essential for providing the outstanding protection desired in a seacoast/seawater environment. Current technology has yet to develop an equivalent method of corrosion protection that does not incorporate the use of chromates. Four systems were found that provided outstanding protection and four additional systems were almost as good. These systems are based on a chromate pretreatment, a chromate epoxy primer and a polyurethane topcoat. Based on the results of this test program, one of these systems should be considered for those applications where superior protection for aluminum surfaces is required. (D. Franklin/EH24/205-453-5872)

## Electron Beam Weld Model

Electron beam welding is a common procedure for joining metals for aerospace and many other applications. The intense heat generated by an electron beam can weld together inch-thick pieces of exotic metals with the apparent ease of closing a zipper. Underlying the apparent ease of this joining process is considerable research into control of the process and avoidance of defects. Welding research carried out at MSFC has produced a computer model of an electron beam weld useful for calculating weld penetration, temperature fields, and weld process efficiencies. The model is also applicable to certain other kinds of welding: gas tungsten arc, plasma arc, and laser beam welding, for example. Weld penetration computations are not new, but so far as is known this model, usable with a small computer, is unique in combining a usefully detailed treatment with the easy operation of a computer game. (A. Nunes, Jr./EH42/205-453-0011)

## Variable Polarity Plasma Arc Welding

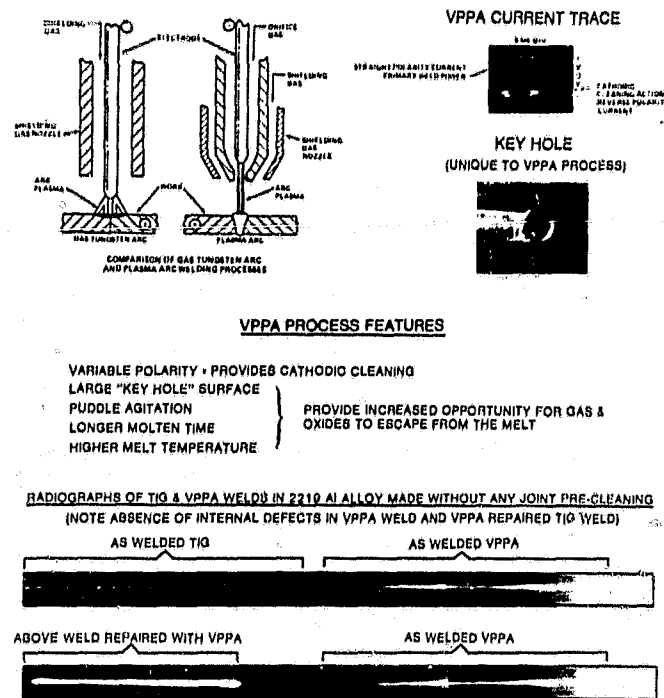


Figure 36. Variable Polarity Plasma Arc Welding

Variable Polarity Plasma Arc (VPPA) for welding aluminum is the most significant process improvement in weld quality since the Gas Tungsten Arc (GTA) process replaced the acetylene torch. The VPPA process reduces the manhours associated with preweld cleaning and reduces the number of repairs for internal defects. This is a relatively new technique which permits plasma keyhole welding aluminum. In this process, the polarity of the weld current is periodically reversed. The straight polarity cycle provides the

principal weld current, while the reverse polarity yields considerable cathodic cleaning action. This cleaning action, and the increased surface area of the weld puddle, i.e., the side walls of the keyhole, removes oxides and other contaminants and allows them to escape to the surface, rather than being trapped within the weld as porosity or oxide inclusions. This process offers considerable promise on the External Tank where preweld cleanliness is difficult to maintain and where joint contamination results in a high number of heat repairs to eliminate internal defects. MSFC is integrating welding equipment into total computer controlled system designed to advance process engineering technology to meet high launch rate fabrication. The control capability is being expanded to include a robot. Figure 36 shows the description of the process. (W. Wilson/EH42/205-453-0011)

#### Micro-Accurate Weld Arc Control Development

By use of new Charge Injection Device (CID) silicon imaging sensors and microprocessor signal processing, a generation of microaccurate, real time, non-surface contact, weld arc guidance controls was developed. Test results, as compared with earlier automatic weld arc guidance controls equipment tested at MSFC, indicate that a higher degree of reliability and accuracy has been achieved. Although the cost of the newly developed system is comparable to earlier weld tracking systems tested, it is substantially more cost effective because the control system is microcomputer controlled, the weld joint illumination is from directly above, and the camera size is vastly reduced and accuracy significantly increased through the use of a digital CID type camera.

The system has a video output for a remote monitor. This monitor is used for prealignment, illumination setup, and to monitor the weld seam tracking. The video monitor, equipped with a calibrated reticle, is extremely useful for real time, or taped playback, quality control verification. Software capability exists for replay of weld joints for multipass welding purposes. The tracking system has been tested and verified with butt and V-groove weld joints. By analysis, the systems should apply to lap joints. However, fillet weld joints require as yet undefined, special preparations to obtain an adequate tracking signal. (W. Wall/EH15/205-453-4878)

#### Detection of Residual Silicone Contaminants on Bonding Surfaces

Trace amounts of silicone contamination on Shuttle hardware subjected to subsequent fabrication procedures and coating processes can drastically affect the quality of any bonding operation. Failure modes include partial debonding over contaminated areas, total debond, or failure to form a bond at all. Bonding between the substrate and the thermal protection coating, that is spray applied to the External Tank, is particularly sensitive to low levels of silicone contamination. Since a cork-filled trowelable silicone formulation is used as a thermal control coating on one part of the External Tank, the potential exists for cross-contamination of areas that will later

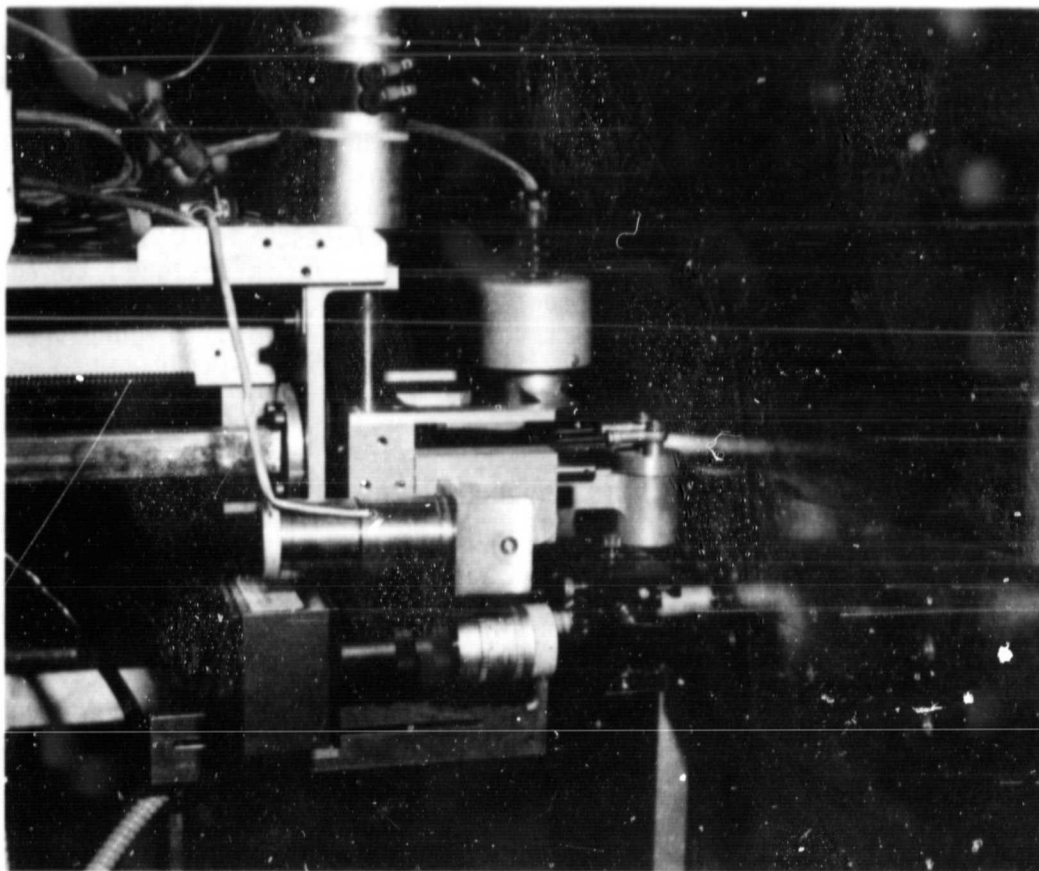


Figure 37. Weld Arc Control with CID Sensor

be sprayed with other coating systems. Trace amounts of silicone, too minute for normal methods of detection and impervious to routine solvent cleaning techniques, have caused costly delays in hardware processing.

An instrument based on photoelectron emission (PEE) characteristics of the epoxy painted substrate has been developed to allow computer controlled scanning of the External Tank or recovered SRB hardware surfaces for silicone or other trace contamination prior to spray application of thermal control coatings. The method is applicable at normal atmospheric pressure under ambient shop conditions, and does not require a vacuum environment characteristic of many spectrographic surface analysis techniques. Instrumentation consists of a ultraviolet source coupled with an electrometer to indicate flux of photoelectron emission from the epoxy painted test surface. Surface contamination is reflected in the attenuation of photoelectron emission level, displayed on the electrometer digital readout. For any particular bonding or spray application process, a PEE acceptance "window" can be established as a guide to surface acceptability. (W. Hill/EH43/205-0643)

## ELECTRICAL POWER TECHNOLOGY

### Power System Automation

Advancements in power system automation techniques were made with the development of two controller breadboard concepts and several power system element algorithms. The breadboard developments included the load center controller and the power subsystem controller. Both controllers utilize the TI SBP9900 as the central processor with communications between the controllers accomplished via a bit-oriented protocol data bus based on the International Standards Organization's standard for high-level data-link control. Algorithms developed include  $NiH_2$  battery state-of-health, energy balance, load shedding, load prioritization, and switch gear fault interrogation. This work was done for MSFC by TRW, Inc. (J. Graves/EC12/205-453-2514)

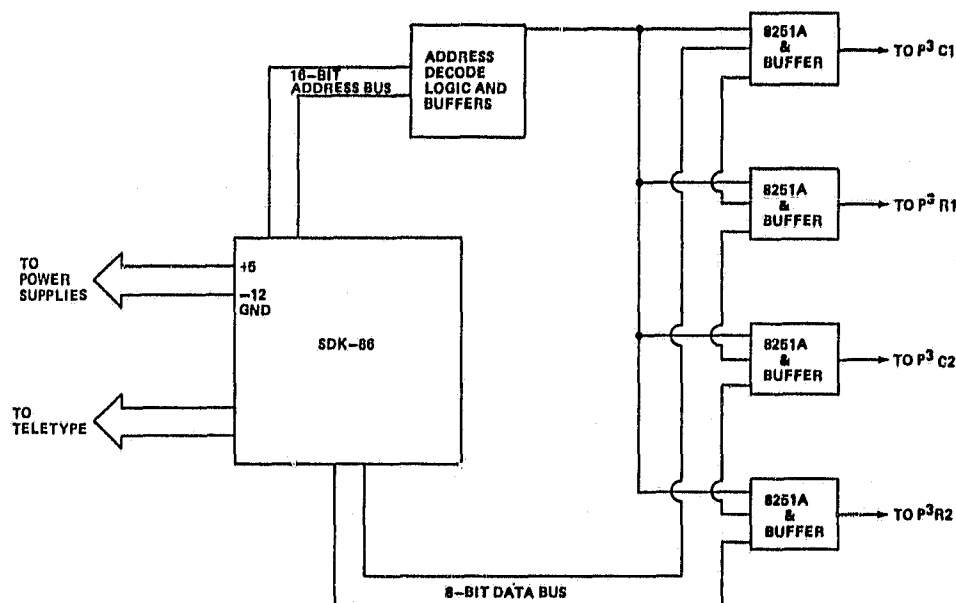


Figure 38. Power System Controller Block Diagram

### Power System Controller for Large Space Electrical Power Systems

With the need for autonomous control of large electrical power systems emerging, a task was undertaken to develop technology for a fail-operational Power System Controller (PSC) utilizing microprocessor technology for managing the distribution and power processor subsystems of a large multi-kW space Electrical Power System. The task involved determining the specific



functions which must be performed by the PSC, determining the best micro-processor available to do the job, and determining the feasibility, cost savings, and applications of a PSC.

Using the INTEL-8086 microprocessor as a baseline, a limited function breadboard version (Figure 38) was developed to demonstrate the concept and potential cost savings by interfacing four Programmable Power Processors to a single command and a data port. (J. Lanier, Jr./EC12/205-453-2113)

### High Voltage Battery

A high voltage battery was developed by MSFC during this year that demonstrated the capability of being employed in high powered aerospace applications, such as the 12 kW Space Platform. It has 110 nickel/cadmium cells in series and is assembled in modules of 22 cells each to provide flexibility in handling. Also incorporated in the design was a BPRC (Battery Protection and Reconditioning Circuit). A diode matrix and toroidal coil for the BPRC has been mounted on each module with the electronics being installed in a separate assembly. The BPRC demonstrated capability of supporting several weak cells during cyclic operation as needed to hold the discharge voltage of those cells above 0.9 volts (as compared with the current average end-of-discharge value of 1.2 volts or higher). Reversal of cells was also prevented during deep discharge by the BPRC circuit.

Approximately 1800 simulated low earth orbit cycles have been performed on two of these batteries operating in parallel. Methods of optimizing charge/discharge requirements are being evaluated through further battery operational tests and engineering studies. (L. Paschal/EC12/205- 453-2111)

Paschal, L. E.: High Voltage Battery Evaluation Program. Presented at the Interagency Advanced Power Group Conference, February 1980.

Lanier, R. L., Jr., Kapustka, R. E., and Bush, J. R., Jr.: A Programmable Power Processor for a 25 kW Power Module. NASA TM 78215, January 1979.

### Thermophotovoltaics

This past year a thermophotovoltaics concept for efficiently converting solar energy to electrical energy was evaluated from an analytical and an experimental approach to prove concept feasibility. A model of a single thermophotovoltaic element is shown in Figure 39. Emphasis this past year was placed upon the experimental analysis. The major components for an experimental system model were evaluated and tested in vacuum, thermal, and radiation. This work is being conducted in conjunction with the Boeing Aerospace Company in an effort to improve efficiency and reduce cost of photovoltaic solar arrays. (W. Crabtree/EC12/205-453-4642)

Horne, E.: Solar Thermophotovoltaic Space Power System. Presented at the IEEE Intersociety Energy Conversion Conference, August 1981.

ORIGINAL PAGE  
BLACK AND WHITE PHOTOGRAPH

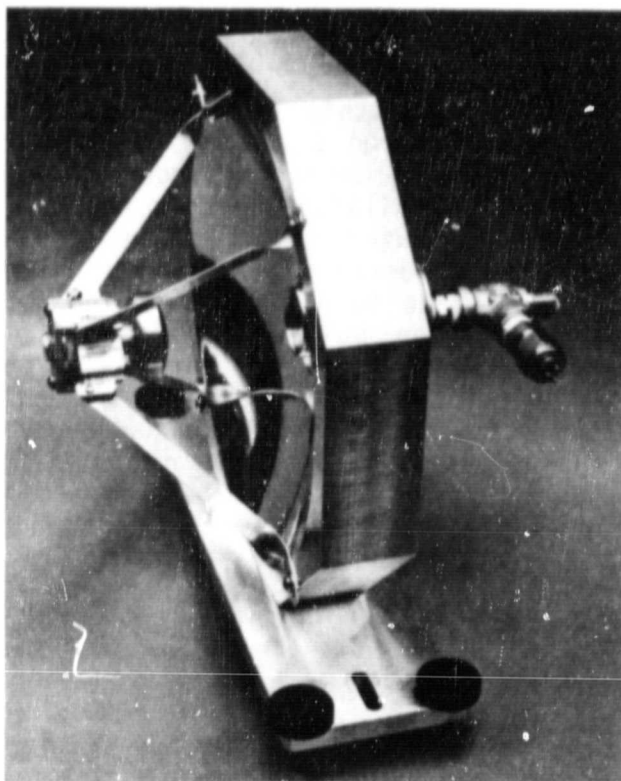


Figure 39. Thermophotovoltaic Generator Module

#### Solar Cell Characterization

One hundred and eighty-six high performance silicon solar cells were characterized for their low temperature low intensity (LTLI) performance in support of SEPS deep space missions. These cells were tested individually under light levels between 0.04 and 1.0 solar constant and in the dark as forward-biased rectifiers and at temperatures ranging from +65°C to -175°C. While all cells demonstrated high performance at 1 SC and 25°C, some cells of all types manifested reduced outputs under LTLI conditions. This reduced performance is attributed to ohmic and rectifying shunt defects introduced into the cells during the manufacturing process. (A. Whitaker/EH12/205-453-4877)

Whitaker, A. F., Little, S. A., et al.: Current-Voltage Characteristics of Spectrolab Sculptured BSR/P<sup>+</sup> (K6.5) and BSR (K4.5) Cells as a Function of Temperature and Intensity. Characterization of Three Types of Silicon Solar Cells for SEPS Deep Space Missions, Vol. III, NASA TM-78305, August 1980.

Whitaker, A. F., Little, S. A.: Solar Cell Performance at Low Illumination and Temperature for Deep Space Applications. J. of Energy, AIAA (submitted).

## ELECTRONICS

### High Density Electronics

It has been predicted that within the next few years 400,000 devices (transistors) will be implemented on a single microelectronic chip. At this level of integration, traditional design procedures using devices or logic gates (NANDs, etc.) as design building elements become impractical. Since 1979 MSFC as part of its Computer Aided Design and Test (CADAT) System development has embarked on a research effort in conjunction with the University of Alabama in Huntsville to implement a high level Hardware Design Language (HDL) where the design building elements are registers, memory blocks, boolean equations, and others. Specific progress achieved in FY81 was the definition of HDL syntax processed by HDL translator software, the adaptation of simulator software which allows coarse checkout of the design early in the design cycle, and synthesis software that implements the design in terms of logic gates in a format compatible with existing CADAT software. This work has been performed by the University of Alabama in Huntsville under contract to MSFC. (J. Gould/EC45/205-453-3772)

Contractor Report: Design Synthesis of Digital Systems. October 1980

### Interactive Color Graphics Design

An interactive color graphics design station is used to design, layout and verify high density microelectronic circuit layouts. It features a graphics software package with unique properties developed for this task. During FY81, MSFC enhanced the graphics software such that it will be practical for the user to interact with the enormous data base resulting from VLSIC layouts. This has been done through the development of an attribute system. It is a technique for classifying the various design items that form the layout. The classification is done by assigning a unique attribute word to each design item and then storing the item in a highly structured data base such that items having the same attribute word are grouped together. By noting the location of these groups, processing can be accomplished quickly even though the design data base is extremely large. (Figure 41). This work was performed by Espee, Inc. (J. Gould/EC45/205-453-3773)

Final Report, Contract # NAS-8-33985: Capability Enhancement of the Artwork Interactive Design System (AIDS), Parts I, II, and III, August 7, 1981.

### Optical Array Sensor

An optical array sensor has been developed for MSFC by the University of Arizona to measure lightning intensity and cloud top brightness from high altitude aircraft. The sensor utilizes a 50 x 50 element silicone photo-sensor array. Various narrow-band optical filters can be mounted in front of the array to take advantage of strong lightning emissions in the near IR (approximately 7700 - 8700 nm). The sensor is calibrated to measure

ORIGINAL PAGE  
BLACK AND WHITE PHOTOGRAPH



Figure 40. High Speed Interactive Color Graphic Design Station

absolute intensity of individual lightning flashes and light reflected from the cloud tops. The sensor field of view is approximately one steradian. It was flown on a NASA U-2 aircraft during the summer of 1981, on both day and night flights. Data reduction is underway and will be completed by the end of 1982. (T. Barnes/EC35/205-453-1574)

#### Three Phase Responsive Motor Controller

The three phase Responsive Motor Controller is a new method for controlling the voltage applied to a three phase induction motor. The system responds to the magnitude of the motor current, continuously adjusting the voltage applied to the motor as the load varies so as to reduce power consumption when the motor is idling or operating at less than full load. The circuit is simpler and less expensive than phase sensing-power factor controllers. This makes it feasible to equip small, modestly used three phase motors with a "Power Saver" whose initial cost can be returned in a minimum of use time by reducing unnecessary energy waste. (T. Edge/EC45/205-453-3766)

### Ground Loop Opto-Isolation

The Communications facilities at MSFC are dispersed over an area of 1,841 acres. Communication systems within the center are all routed through Central Communications, Building 4207. Different system configurations often create extremely long cable runs between buildings. As the distance increases, the cable resistance also increases, and at times a substantial difference of potential between input and output devices will develop. This problem is further complicated by the fact that the primary power network for the Center is also dispersed over a large area. Ground loop voltages of up to 2 V are sometimes superimposed on signals of less than one volt. A means of eliminating this ground loop was required. Differential amplification was not satisfactory, for this merely passed the 60 Hz hum along with the desired signal. The successful solution to this problem was to optically couple the system inputs and outputs. Circuits were fabricated that were, in most cases, relatively simple and that properly terminated the transmission line. The resulting isolation improved the immunity of the system to differential-mode-noise. Linearity can be improved at the expense of signal-to-noise ratio. Both linearity and signal-to-noise ratio are fairly sensitive to power supply stability. The circuit must be placed at the point where the ground loop is induced, in order to provide the desired isolation. (E. Hildreth/AB51/205-453-3470)

### Superconductivity Research

#### Readout Circuitry for the GP-B Experiment

Advanced research and development were accomplished toward meeting the requirements for the Gravity Probe-B (GP-B) experiment proposed by Stanford University. Some of the main areas include: coating a fused silica gyro rotor uniformly with a niobium film that will be superconducting, measuring the uniformity of this film with great precision, fabricating superconducting readout loops on a gyro housing half, and examining the characteristics of optically contacted surfaces at liquid helium temperatures (needed as a stable construction technique for the gyro). A coating uniformity to within 7.5 nm (0.3 microinch) has been specified as a goal, and a film of 2500 nm (approximately 100 microinch) thickness is desirable for ground testing purposes.

Superconducting films have been produced by sputtering; uniformities to approximately 3 percent in 2500 nm films have been obtained by manipulation of the rotor while coating it on an argon gas bearing. Relatively poor reproducibility was obtained; either use of a thinner-than-desirable film or improved coating techniques will be required. Numerous problems associated with mechanically rolling a rotor during coating were solved. A second-generation mechanical roller system has been designed and is under construction which will utilize microprocessor control to position the rotor to many orientations during sputtering. This system is expected to provide reproducible coatings and improved uniformities.

A prototype readout circuit for the gyro was fabricated using niobium films, negative photoresists, a focused laser beam, programmed microprocessor-controlled stages, and sputter etching. Characteristics of several type of contracts for use as superconducting connector terminals were examined by a faculty member from South Carolina State College while on the 1981 NASA-ASEE Summer Faculty Fellowship program. These contacts are being considered for readout circuitry applications.

The tensile strengths of a number of optically contacted fused silica surfaces were measured at 4.2°K. The results indicate that strengths in excess of 650 psi are possible, and the bonds appear to be stronger at 4.2°K than at 300°K. Another faculty member from South Carolina State College assisted with these measurements while on the same program. (P. Peters/ES63/205-453-5134)

### Evaluation and Analysis of Superconducting Composites

The objective was to characterize the superconducting properties of directionally solidified materials to relate these properties to microstructure, macrostructure, and processing parameters. The original objectives were successfully accomplished and include: (1) the pertinent processing parameters necessary for fabrication of specific composite materials by directional solidification techniques. The accomplishment of this task required developing a new technique for initial dispersion of niobium within a copper matrix. Subsequent directional solidification can be used to produce composite structures. (2) Resistivity measurements were performed on selected samples from room temperature to liquid helium and the results indicated that the aligned structure was effectively a continuous medium conducive to providing a superconductive path through the composite. (3) The resistivity samples were wire sections drawn from the original castings, directionally solidified, tin plated, thermally treated, and tested. This processing should produce a Nb<sub>3</sub>Sn compound having a critical temperature T<sub>c</sub> of 18°K. Samples have been provided to the University of Alabama in Huntsville for T<sub>c</sub> measurements. The investigations completed on aligned miscibility gap materials confirm that the objectives for this program are achievable. Additional expertise in low temperature physics is necessary to evaluate electrical properties of the superconductivity materials produced by this technique. (M. Johnston/EH22/205-453-5510)